

Thesis for the Degree of Doctor of Philosophy

Analytical Models for Optimizing Transmission Efficiency in Hierarchical Wireless Networks

Zilong Jin

Department of Computer Engineering
Graduate School
Kyung Hee University
Seoul, Korea

February, 2016

Analytical Models for Optimizing Transmission Efficiency in Hierarchical Wireless Networks

Zilong Jin

**Department of Computer Engineering
Graduate School
Kyung Hee University
Seoul, Korea**

February, 2016

Analytical Models for Optimizing Transmission Efficiency in Hierarchical Wireless Networks

by
Zilong Jin

Supervised by
Prof. Jinsung Cho, Ph.D.

Submitted to the Department of Computer Engineering
and the Faculty of the Graduate School of
Kyung Hee University in partial fulfillment
of the requirements for the degree of
Doctor of Philosophy

Dissertation Committee:

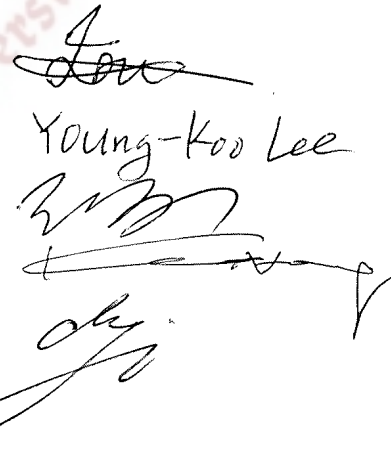
Prof. Sungwon Lee, Ph.D. (Chairman)

Prof. Young-Koo Lee, Ph.D.

Prof. Seokhee Jeon, Ph.D.

Prof. Een-Kee Hong, Ph.D.

Prof. Jinsung Cho, Ph.D.



Young-Koo Lee

Abstract

The hierarchical structure has been adopted as an efficient solution for designing wireless communication systems to achieve economic construction and operation. The hierarchical structure is also a useful way for designing a reliable wireless network, because it breaks the complex problem of network design into smaller and more manageable areas. A three-level hierarchy structure is widely applied in emerging communication systems, such as relay networks and cluster-based Wireless Sensor Networks (WSN).

For the wireless networks, how to design an efficient hierarchy structure is arisen as an important research topic. In relay networks, the designing problem of hierarchical structure can be regard as answering the question that “How many Relay Stations (RSs) should be deployed?” which significantly affects the network deployment and operating cost. In the cluster-based WSN, the designing problem of hierarchical structure comes down to optimizing the network Cluster Ratio (CR) because improper number of CR results in increasing the network communication overhead and the energy consumption.

For the designing efficient hierarchical wireless networks, analytic models which are developed based on the stochastic properties of the networks will be an efficient way to minimize the planning cost. However, there are a lot of characterizes of the hierarchy networks should be taken into account to precisely analyze the impact of the network structure on the network performance. For example, terrain influence, signal propagation environment, QoS requirement and the network constraints. Although the comprehensive parameters are helpful for increasing the accuracy of estimation results, it increases

the analysis complexity in terms of calculation and hypothesis. With the comprehensive parameters, the optimal results will be generated by the development of a complex programming, and it should be adapted to each practical network structure. Therefore, an analytic model with comprehensive parameters is not feasible in the three-level hierarchy networks, and it will result in restriction of candidate applications.

In this thesis, the above mentioned challengers for developing efficient analytic models are addressed. Specifically, the developed analytic models are efficient to optimize transmission efficiency of the three-level hierarchy networks in terms of the networks' costs and energy efficiency. The analytic models also address the design of the public network structure, and incorporates more generalized constraints to allow the network planner a higher degree of freedom in planning the network deployment and structure on local requirements. In order to guarantee the analytic models' applicability, the hypothesis parameters are limited through mathematically modeling the networks. Furthermore, the common characteristic of spatial structure of the three-level hierarchy networks is taken into account in the analytic models to normalize the analyses.

Besides the above mentioned common contributions, the specific achievement are summarized in two parts.

First, this thesis presents an analytic model to describe the impact of the number of RSs on the channel capacity of relay networks. From the mathematical analysis, the optimal number of RSs is obtained to satisfy QoS requirements of users considering various levels of MCS (Modulation and Coding Scheme). In addition to the mathematical analysis, we also examine its performance through a set of simulations. The simulation results show the validity of the proposed analytic model.

Second, this thesis analyzes the optimal cluster ratio from the perspective of network energy efficiency. In order to provide a generic analytic model, various data propagation cases are mathematically analyzed. Furthermore, the network lifetime is extended by jointly optimizing the network transmission count and link reliability. Our simulation

results show that the optimal cluster ratio derived based on the proposed analytical model enhances energy efficiency and effectively increases the network lifetime.



Acknowledgment

First and foremost I would like to thank my advisor Prof. Jinsung Cho, not only for his tremendous academic support, but also for giving me so many wonderful opportunities and encouragements. Under his guidance, I successfully overcame many difficulties and learned a lot. I hope that one day I would become as good an advisor to my students as Prof. Jinsung Cho has been to me. I also warmly thank Prof. Ben Lee for his valuable advice, constructive criticism and his extensive discussions around my work.

My sincere thanks goes to the members of my PhD Committee, Prof. Sungwon Lee, Young-Koo Lee, Seokhee Jeon, and Een-Kee Hong, for their encouragement and insightful comments.

I am also grateful to the current and past members of mobile & embedded system lab. Particularly, I would like to acknowledge Dr. Dae-young Kim and Dr. Choongyoung Shin for the many valuable discussions that helped me understand my research area better. I am indebted to friendly and cheerful members; Sangbae Shin, Daehoon Kim, Yoonjeong Han, Weidong Su, Sunghyun Kim, Kyunryun Cho, Jonghyun Choi, Jieun Lee, and Fanhua Kong, who made me have an unforgettable experience in Korea.

Many friends have helped me stay happy through these difficult years. I appreciate Yuhui Zheng, Jingyuan Li, Peixin Li, Yunfei Wu, Peng Zhang, and Xing Fu; without their support and care it is impossible to overcome setbacks and stay focused on my graduate study. A special thanks goes to Dr. Donghai Guan and Dr. Weiwei Yuan for their motivation and encouragement. Dr. Donghai Guan is a life mentor to me. He has

been always there to listen and give advice, and I have learnt much from and because of him in many ways.

Last but not the least, I would like to dedicate this thesis to my family and my wife, Siyu, for their love, support, and inspiration. This accomplishment would not have been possible without them. Thank you.

Zilong Jin

Dec. 28, 2015

Yongin, Korea



Table of Contents

| | |
|--|-------------|
| Abstract | i |
| Acknowledgment | iv |
| Table of Contents | vi |
| List of Figures | viii |
| List of Tables | xi |
| Chapter 1 Motivation, Contributions, and Organization | 1 |
| 1.1 Motivation | 1 |
| 1.2 Contributions | 4 |
| 1.2.1 Optimizing the Hierarchical Structure in Relay Networks | 4 |
| 1.2.2 Optimizing the Hierarchical Structure in Cluster-based Wireless Sensor Networks | 5 |
| 1.3 Organization | 7 |
| Chapter 2 Background and Related Work | 9 |
| 2.1 Background | 9 |
| 2.1.1 Hierarchical Structure for Wireless Networks | 9 |
| 2.1.2 Relay Networks | 11 |
| 2.1.3 Cluster-based Wireless Sensor Networks | 13 |

| | | |
|------------------|--|-----------|
| 2.2 | Related Work | 14 |
| 2.2.1 | Analytic Models for Relay Networks | 14 |
| 2.2.2 | Analytic Models for Cluster-based Wireless Sensor Networks | 16 |
| Chapter 3 | Network Model | 19 |
| 3.1 | Relay Networks | 19 |
| 3.1.1 | Relay Model | 19 |
| 3.1.2 | Signal Propagation Model | 20 |
| 3.2 | Cluster-based Wireless Sensor Networks | 23 |
| 3.2.1 | Cluster Model | 23 |
| 3.2.2 | Signal Propagation Model | 23 |
| 3.2.3 | Data Propagation Model | 24 |
| Chapter 4 | Analytic Model for Optimizing Cost Efficiency in Relay Networks | 27 |
| 4.1 | Overview | 27 |
| 4.2 | Analysis on the Optimal Network Structure | 28 |
| 4.2.1 | Analysis on Stochastic Geometry in the Relay Station Served Region | 29 |
| 4.2.2 | Evaluating Channel Capacity of Relay Stations | 30 |
| 4.2.3 | Analytic Model for Optimizing the Number of Relay Stations | 32 |
| 4.3 | Performance Evaluation | 33 |
| 4.3.1 | Validation of the Approximation Efficiency | 33 |
| 4.3.2 | Performance of the Proposed Analytic Model | 34 |
| 4.4 | Summary | 36 |
| Chapter 5 | Analytic Model for Optimizing Energy Efficiency in Cluster-based Wireless Sensor Networks | 38 |
| 5.1 | Overview | 38 |

| | | |
|------------------|--|-----------|
| 5.2 | Analysis on the Optimal Network Structure | 39 |
| 5.2.1 | Optimal Cluster Ratio for Minimizing Inherent Transmission Count | 40 |
| 5.2.2 | Optimal Cluster Ratio for Maximizing Communication Reliability | 46 |
| 5.2.3 | Joint Optimization | 48 |
| 5.3 | Performance Evaluation | 51 |
| 5.3.1 | Validation of the Approximation Efficiency | 52 |
| 5.3.2 | Performance of the Proposed Joint Optimization | 55 |
| 5.3.3 | Comparison with Existing Analytic Models | 56 |
| 5.3.4 | Network Life Time | 59 |
| 5.4 | Summary | 61 |
| Chapter 6 | Conclusions and Future Work | 63 |
| 6.1 | Conclusions | 63 |
| 6.2 | Future Work | 64 |
| | Bibliography | 66 |
| | Appendix A Proof of Formula (5.2) | 74 |

List of Figures

| | | |
|-----|---|----|
| 1.1 | An example of three-level hierarchy network. | 3 |
| 2.1 | A simplified three-level hierarchy structure | 10 |
| 2.2 | Example of usage scenarios for RSs | 12 |
| 3.1 | Signal propagation cases | 22 |
| 3.2 | Data propagation models | 25 |
| 4.1 | Numerical analysis and simulation results | 34 |
| 4.2 | Average path loss analysis in a cluster | 35 |
| 4.3 | Spectral efficiency with different number of RSs | 36 |
| 5.1 | The impact of Cluster Ratio on normalized ITC and PRR ($k = 3.3$ and $r_{min} = 10$ m) | 45 |
| 5.2 | Results of joint optimization | 50 |
| 5.3 | Comparison of simulation and approximation results ($r_{min}=10$ m and $p = \{0.08, 0.12, 0.16, 0.2, 0.24\}$) | 52 |
| 5.4 | Comparison of the network ITC for different node densities | 56 |
| 5.5 | Comparison of the average PRR for different node densities | 57 |
| 5.6 | Network ITC | 58 |
| 5.7 | Average PRR | 59 |
| 5.8 | Average energy consumption | 60 |

| | | |
|-----|--------------------------------------|----|
| 5.9 | Received packet before FND | 61 |
|-----|--------------------------------------|----|



List of Tables

| | | |
|-----|---|----|
| 3.1 | Path loss types for IEEE 802.16j based relay networks | 21 |
| 3.2 | Parameters for different terrain Type A/B/C | 21 |
| 4.1 | Parameter notation and definition | 31 |
| 5.1 | Bit error probabilities for modulations | 47 |
| 5.2 | Data comparison: Number of nodes deployed is 400 | 51 |
| 5.3 | Data comparison: Number of nodes deployed is 500 | 53 |
| 5.4 | Data comparison: Number of nodes deployed is 600 | 53 |
| 5.5 | RMSE for different environments | 55 |

Chapter 1

Motivation, Contributions, and Organization

1.1 Motivation

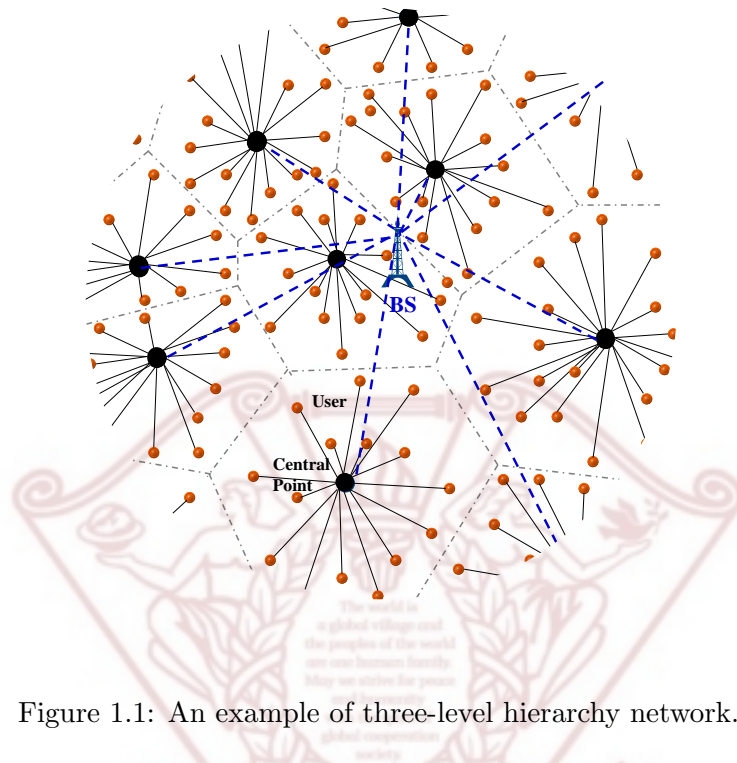
In the past few decades, a hierarchical structure was designed for telecommunication systems to achieve economic construction and operation [1]. The hierarchical structure is also a useful way for designing a reliable network, because it breaks the complex problem of network design into smaller and more manageable areas. The basic ideas behind the hierarchical network structure can be traced back to the third-generation (3G) wireless networks. In the networks, by managing the network with several levels of hierarchy, both of the frequency reuse distance and the handoff overhead are reduced, and thus the network capacity is increased [2]. A two-level hierarchy is a popular structure in telecommunication systems. For example, in cellular networks, the higher level indicates the Base Station (BS) which is connected with the backbone network. The lower level consists of a set of user nodes which are served by the BS.

A three-level hierarchy structure is also widely applied in emerging communication systems, i.e., relay networks and cluster-based WSN (Wireless Sensor Networks). In the relay networks, the first two hierarchies are similar with the two-level hierarchy telecommunication system. As shown in Figure 1.1, the additional hierarchy in the relay network consists Relay Stations (RS) and user nodes. The RS is a new entity in wireless networks, i.e., cellular networks, ad-hoc networks, sensor networks, and mesh

networks, and introduced to form virtual antenna arrays to achieve some benefits such as diversity gains [3]. User nodes will select a RS based on a certain selection criterion. The selection criterion can be designed according to the systems' restrictions and users' requirements. The nearest-neighbor RS selection scheme is the most popular one in the relay transmissions because it has low overhead and similar capacity gain compared with other complicated RS selection schemes [4]. According to the RS selection scheme, the user nodes join the nearest to them RS and the whole network is separated by several convex polygons. The same characteristic of the spatial structure can be found in cluster-based WSNs. In cluster-based WSNs, the network contains several clusters and each cluster is managed by a Cluster Head (CH). The CHs are selected based on a predetermined Cluster Ratio (CR). In addition to CHs, the other nodes, called Cluster Members (CMs), join the CH that is closest to them.

Due to the characteristic of the spatial structure of the three-level hierarchy networks, the sub-central point play a key role in the networks. In relay networks, a RS cooperates with user nodes which are served by the RS and increases the channel capacity of the user nodes. In the cluster-based WSN, clustering schemes can decrease the amount of transmitted traffic at a CH using data aggregation, and thus energy can be saved during data transmission. In addition, since nodes are managed as a cluster, the network becomes more robust and the overhead due to frequent topology changes is reduced. However, in these three-level hierarchy networks, there are a set of studies indicated that the improper choice of the number of sub-central points, i.e., RSs and CHs, can result in bottleneck problem at the sub-central points in relay networks and decrease the energy efficiency in the cluster-based WSNs.

Therefore, analytic models which can be utilized for efficiently analyzing the impact of sub-central points on the network transmission efficiency in terms of the network costs and energy efficiency arise as an important research topic to construct effective three-level hierarchy networks with minimum network planning cost. There are a lot of characterizes



of the hierarchy networks should be taken into account to precisely analyze the network. For example, terrain influence, signal propagation environment, QoS requirement and network constraints. The comprehensive parameters are helpful for increasing accuracy of estimation results. On the other hand, it also increases the analysis complexity in terms of calculation and hypothesis. The optimal results will be generated by developing a complex programming, and it should be adapted to each practical network structure. Therefore, an analytic model takes into account comprehensive parameters is not feasible in the three-level hierarchy networks, and it will result in restriction of candidate application of the analytic model.

Consequently, feasible analytic models are desired to optimize the three-level hierarchy networks in terms of the networks' costs and performances. The analytic models should address the design of public network structure, and incorporates more generalized constraints to allow the network planner a higher degree of freedom in planning the net-

work deployment and structure on local requirements. In order to guarantee the analytic models' applicability, the hypothesis parameters should be limited. Furthermore, the common characteristic of spatial structure of the three-level hierarchy networks should be taken into account in the analytic models.

1.2 Contributions

In this thesis, we tackle the aforementioned challenges in the development of feasible analytic models for the three-level hierarchy networks. The analytic models are proposed for the emerging three-level hierarchy networks which are the relay network and cluster-based WSN. The main technical solutions and contributions are presented as follows.

1.2.1 Optimizing the Hierarchical Structure in Relay Networks

Relay transmissions have been adopted as a promising solution to achieve high data rates by minimizing the signal fading problem. The basic idea of relay transmission is that multiple RSs are distributed in a cell and each RS with a single antenna can cooperate with others by composing virtual antenna arrays in order to confer benefits similar to those provided by conventional Multiple-Input Multiple-Output (MIMO) systems. As a key concept, a RS is the new entity introduced by relay networks [5]. The RSs are deployed as infrastructure devices without connecting to wired backbone, and serve towards various objectives, such as extending the network coverage, the network capacity and throughput in areas which are not sufficiently covered. When Base Stations (BS) and users broadcast signal, the distributed RSs can receive the signal and relay it to relevant users or BSs.

There are many valuable investigations of practical issues on relay transmissions. Most of these investigations focus on the issue of optimal RS selections and RS assignment. They neglect another important issue related to RS, that is "How many RS we

need to place”. They just randomly choose the number of RS in their schemes. In fact, the optimal number of RS is one of the important preconditions to guarantee the performance of these schemes.

In this thesis, we mathematically analyze the optimal number of RSs for the constructing relay networks. We use a simple RS selection scheme where the nearest RS to the source is selected. Based on that, we analytically evaluate the characteristics of the spatial structure of the networks, and mathematically model the impact of the number of RS on the network optimization in terms of the network cost and performance.

The specific contributions of this research topic are shown as follows [6]:

- The proposed analytic model can be utilized to estimate the optimal number of RSs that can satisfy users’ QoS requirements based on a general assumption that RSs and users are randomly distributed by Poisson point process.
- The Adaptive Modulation and Coding (AMC) scheme is taken into account in the proposed analytic model to guarantee the QoS requirement of the network user.
- The proposed analytic model derives not only the lower bound on the number of RSs but also the optimal number of RSs for various levels of Modulation and Coding Scheme (MCS).

1.2.2 Optimizing the Hierarchical Structure in Cluster-based Wireless Sensor Networks

Clustering schemes have been explored to enhance energy efficiency and communication performance, as well as improve network scalability [7, 8, 9, 10, 11]. Clustering schemes in WSNs can decrease the amount of transmitted traffic at a Cluster Head (CH) using data aggregation, and thus energy can be saved during data transmission [12]. In addition, since nodes are managed as a cluster, the network becomes more robust and the overhead due to frequent topology changes is reduced.

Prior research efforts in cluster-based WSNs [13], [14], [15], [16], [17], indicate the importance of Cluster Ratio (CR), which is the ratio of the number of cluster-heads and the total number of nodes. These studies found that an improper choice of CR will result in extra energy dissipation, and thus an appropriate choice of CR is critical for enhancing the network lifetime. However, their results are only based on specific environments and transmission cases, and thus not applicable for general cluster-based WSNs. For example, Yang and Sikdar [14] and Chen *et al.* [18] proposed analytical models to determine the optimal CR, but they do not consider multi-hop transmissions. Xie and Jia [17] mathematically analyzed the optimal CR for minimizing the number of network transmissions. Their analysis was performed based on the assumption that the network is divided into uniform sized clusters. However, this is not the case in most WSN applications, where the location and shape of each cluster are random. Consequently, there are no valid analytical models that can be applied using generic assumptions and various data propagation cases.

In order to propose a feasible analytic models for the networks, the characteristic of the spatial structure is firstly analyzed in the cluster-based WSN, and then the relationship between CR and network performance is analyzed for improving the network energy efficiency. The analytic model is achieved by modeling a cluster-based WSN as a 2-dimensional Poisson point process and analyzing the impact of CR on the network performance in terms of transmission count and *Packet Reception Ratio (PRR)*. Finally, a joint optimization scheme is proposed to derive the optimized CR that guarantees network energy efficiency and prolongs network lifetime.

The specific contributions of this research topic are shown as follows [19]:

- The impact of CR on the network performance is mathematically analyzed in terms of transmission count and communication reliability.
- The optimal CR is analyzed for a generic and feasible network environment as well

as various data propagation cases. This allows the proposed analytic model and the result of optimal CR to be widely applied in cluster-based WSNs.

- An important **Theorem** and an accompanying proof are provided to show that the inherent transmission count of a cluster-based WSN is a **Convex Function** of CR . (The definition for inherent transmission count will be given in Sec. 5.2.1.) This property indicates that the network energy efficiency can be guaranteed by optimizing CR .
- A joint optimization is performed to simultaneously optimize transmission count and PRR . The optimized results are verified using simulation.

1.3 Organization

The rest of the thesis is organized as follows:

Chapter 2: Background and Related Work. In this chapter, we first briefly introduce the three-level hierarchy networks, and describe background for relay networks and cluster-based WSN. Then we discuss existing analytic models for the three-level hierarchy networks and outline differences between the existing efforts and proposed methodologies.

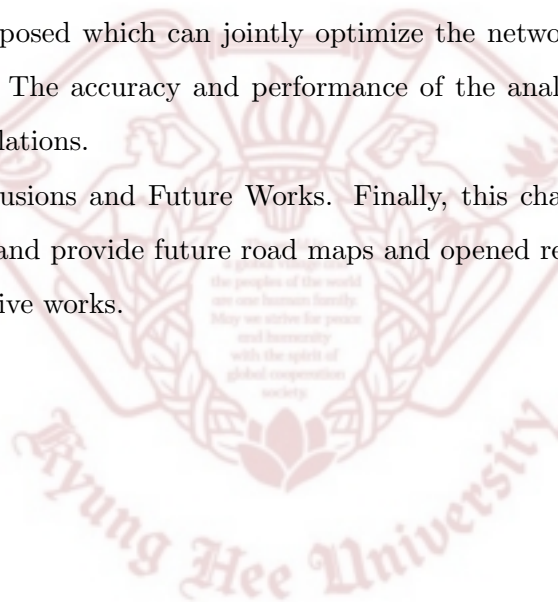
Chapter 3: Network Model. This chapter presents the basic assumptions for the considered hierarchical networks. One of the challenges in developing a feasible analytic model is the analyses complexity and applicability for various network environment. Therefore, this chapter defines a general data propagation model and signal propagation models for the considered hierarchical networks.

Chapter 4: Analytic Model for Optimizing Cost Efficiency in Relay Network. This chapter proposes an analytic model for optimizing cost efficiency of the relay network. First, optimal range of RS is analyzed, and then impact of the number of RSs on the network channel capacity is analyzed. Finally, according to the analyses, the optimal number of RS is proposed for optimizing the network in terms of the network cost and

performance. The accuracy and performance of the analytic model are proved through a set of simulations.

Chapter 5: Analytic Model for Optimizing Energy Efficiency in Cluster-based Wireless Sensor Networks. This chapter takes a deeper analysis on the relation between the hierarchical structure and the network performance in cluster-based WSNs. First, the optimal cluster ratio for minimizing inherent transmission count is analyzed. Then, the optimal cluster ratio for maximizing communication reliability is exploited. Finally, an analytic model is proposed which can jointly optimize the network energy-efficiency in cluster-based WSNs. The accuracy and performance of the analytic model are proved through a set of simulations.

Chapter 6: Conclusions and Future Works. Finally, this chapter concludes contributions of the thesis and provide future road maps and opened research issues from the proposed comprehensive works.



Chapter 2

Background and Related Work

In this chapter, we first briefly introduce the three-level hierarchy networks, and describe background for relay networks and cluster-based WSN. Then we discuss existing analytic models for the three-level hierarchy networks and outline differences between the existing efforts and proposed methodologies.

2.1 Background

2.1.1 Hierarchical Structure for Wireless Networks

Since the current radio bandwidth is lack to guarantee the rapidly increasing requirement of mobile user in telecommunication systems, splitting cells into smaller one is widely applied to improve the network capacity. The reason is that by utilizing the cell splitting, the frequency reuse distance is decreased, and thus the same spectrum band can be reused more times by the mobile users which are away form the issue region and the system capacity is increased.

However, the splitting cell introduces an additional system overhead which is frequent handoff because a mobile user more likely crosses more cells while moving among different places. The hierarchical network structure is an efficient solution for solving the shortcomings of the splitting cell and enhancing the network capacity. A typical three-level hierarchy structure is shown in Fig.2.1. The other advance of the hierarchical structure is also a useful way for designing a reliable network structure, because it breaks

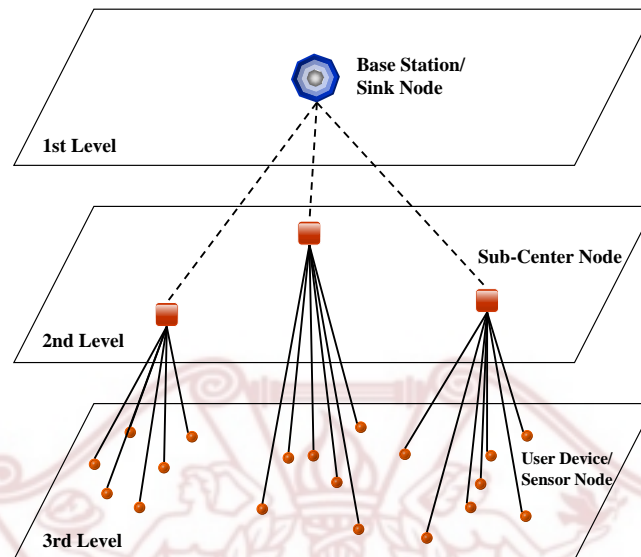


Figure 2.1: A simplified three-level hierarchy structure

the complex problem of network design into smaller and more manageable areas.

In addition to the hierarchical structure plays key role in telecommunication systems, we can also find advantages of the structure in the emerging wireless systems such as the relay network and cluster-based WSN.

In the relay network, the first two hierarchies are similar with the two-level hierarchy telecommunication system. The additional hierarchy in the relay network consists Relay Stations (RS) and user nodes. In the hierarchy, RS utilized to form virtual antenna arrays to achieve some benefits such as diversity gains [3, 20]. Through introducing the hierarchy in which RSs provide additional cooperation between user and BS, the traditional weak links, i.e., user to BS or contrary direction, which suffer low SNR in shadowing and cell-edge areas are cooperated with more strong links that are user/BS to RS and RS to BS/user. In the receiver side (user or BS), the two signals, i.e., received directly and relayed by RS, is combined into a errorless signal based on the spatial diversity. Thus

the performance of the network in terms of capacity and throughput can be significantly enhanced.

The similar three-level hierarchy structure can be found in cluster-based WSNs. In cluster-based WSNs, the network contains several clusters and each cluster is managed by a Cluster Head (CH). The CHs are selected based on a predetermined cluster ratio (CR). In addition to CHs, the other nodes, called Cluster Members (CMs), join the CH that is closest to them. After performing the clustering algorithm, the network is re-structured with three-level. The first level indicates sink nodes which are connected with the Internet or a data center. The second level consists CHs which are connected with sink nodes directly or based on multi-hop. In the third level, sensor nodes communicate with a corresponding CH. The most important advantage of the hierarchical structure in energy restricted WSNs is reducing the communication overhead (which means the number of connections in the network). In a flat network structure, the communication overhead tends to $O(n^2)$ where n is the number of sensor nodes, and thus it makes the flat structure impractical in energy restricted WSNs [21, 22]. The three-level hierarchy structure is helpful for solving this problem because the gathered data in the third-level contains a certain level of redundancy. The CH can perform a data aggregation scheme before transmitting the data to the sink node directly and this process introduces significant advantages as reducing the amount of data traffic, communication overhead, and improving the network energy efficiency.

2.1.2 Relay Networks

Wireless signal fading is one of the major problems for the next generation wireless networks, which require high bandwidth efficiency services. Multiple-Input Multiple-Output (MIMO) system is an advanced technology that can effectively exploit the spatial diversity to solve the problem of signal fading and bring significant performance improvements to wireless communication systems. In order to obtain diversity gain in MIMO system, a

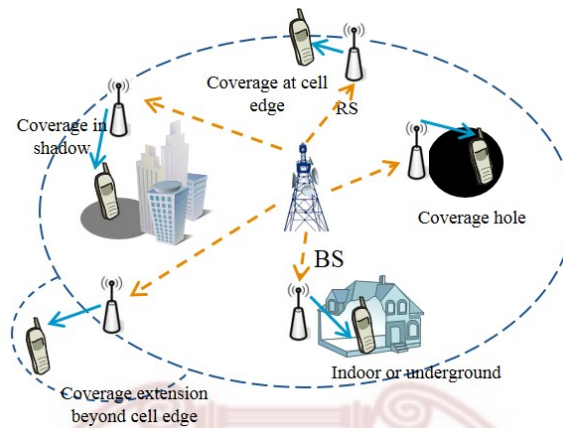


Figure 2.2: Example of usage scenarios for RSs

wireless agent must be set multiple antennas and guarantee at least $\omega/2$ interval between antennas (ω is wavelength) to avoid signal interference. For example, 2.4 GHz frequency band needs at least 6.125 cm interval between antennas. Although the performance of MIMO is quite good, it is suffered from the size limitation of wireless agents. When the size of a wireless agent is small, it may not be able to support multiple transmit antennas.

Relay transmission have been adopted as another promising solution to achieve high data rate by minimizing the signal fading problem. Compared with MIMO, it is no more limited by the size of wireless agents due to its unique idea. The basic idea is that using multiple distributed transceivers, each with a single antenna can cooperate with one another to form virtual antenna arrays, to achieve some benefits similar to those provided by conventional MIMO systems. As a key concept, a RS is the new entity introduced by relay network [5]. Fig. 2.2 shows the examples of usage scenarios for RS. In the Fig. 2.2, the RSs are deployed as infrastructure devices without connecting to wired backbone, and serve towards various objectives, such as improving coverage, capacity, or throughput in areas which are not sufficiently covered. When BSs and users broadcast signal, the distributed RSs can receive the signal and relay it to relevant users or BSs.

2.1.3 Cluster-based Wireless Sensor Networks

In the recent few years, Wireless Sensor Networks (WSN) have been widely applied in various civilian and military applications, for example, environment monitoring, health-care, intrusion detection, battle field surveillance, and industry process control, and play a key role in the Internet of Things (IoT) paradigm. The various applications of WSNs is motivated by the advances in microelectronic-mechanical systems and low-power radio technologies, i.e., ZigBee, low-power Bluetooth, which enable the development of tiny sensor devices and low-cost network construction. Due to utilizing the low-power short-range radio module typically, the communications in WSNs are based on multi-hop. WSNs consists of a large number of tiny sensor nodes each equipped with a microprocessor, a memory, sensing modules, radio transceivers, and a battery. However, in order to minimize the deployment cost and size of sensor nodes, they are equipped with limited battery power.

The limited battery resource result in significant challenges on the energy efficiency of the networks. Therefore, many schemes have been proposed with energy efficiency in mind, such as energy efficient Media Access Control (MAC) and routing schemes. Furthermore, some research efforts have been made on exploring energy efficient network structures [7, 8, 9, 10, 11, 13]. They were inspired by the characteristic of data which is gather by the sensor nodes. Specifically, due to the network is densely deployed, the gather data are closely correlated with the data from its neighbor nodes [23]. And some research efforts indicated that the energy consumption of transmitting one bit to 100m away is the same with processing 3000 instructions [24]. Thus, performing the data aggregation before transmitting it to the sink node directly introduces significant advantages as reducing the amount of data traffic and improving the network energy efficiency [18, 25]. The data aggregation can be achieved by adjusting the network structure with clustering schemes.

Heinzelman *et al.* proposed a cluster-based communication protocol called Low-

Energy Adaptive Clustering Hierarchy (LEACH) [13], which is the most well-known clustering scheme for WSNs. Recently, clustering schemes have been explored to enhance energy efficiency and communication performance, as well as promote the practical deployment and application of WSNs.

The network structure configured based on the cluster schemes is called cluster-based WSN. The network contains several clusters and each cluster is managed by a *Cluster Head* (CH). The CHs are selected based on a predetermined *CR*. In addition to CHs, the other nodes, called *Cluster Members* (CMs), join the CH that is closest to them. After establishing the clusters, CMs collect data based on event-driven and/or predetermined time period from the point in a region of interest. Then CMs send the data to cluster heads, and after performing data aggregation, CHs send the aggregated data to the sink node.

2.2 Related Work

2.2.1 Analytic Models for Relay Networks

IEEE 802.16j multi-hop relay network task group, which was created in March 2006, aims to develop low-cost relay infrastructure architectures for IEEE 802.16 systems [26]. In IEEE 802.16j, RSs are effectively utilized in several scenarios such as cell coverage extension, decreasing shadows area, and enhancing channel capacity.

Related works on optimal utilization of RSs can be classified into two categories: RS selection and RS deployment. A lot of works focused around optimal RS selection issues in relay transmissions [27, 28, 29, 30, 31, 32, 33]. Li *et al.* proposed a centralized optimal RS selection scheme [27]. The optimal RS is selected according to a weight value which is calculated by SNR (Signal to Noise Ratio) and latency. Kadloor *et al.* used the sum rate as a factor and develop a convex optimization problem that provides a tight upper-bound [28], and in [29] a linear marking mechanism was used to minimize

algorithm complexities. The remaining works [30, 31, 32, 33] assumed that the channel fading is slow enough, and thus, current channel state can be used to predicate next one. Then the optimal RSs are selected through defining various selection criteria which are based on physical layer or other layer parameters. However, Wei *et al.* indicated that the assumption is not realistic in nature of mobile environments [34]. They not only analyzed channel variations quantitatively but also proposed a finite-state Markov channel model based RS selection scheme which outperforms existing memoryless and random selection schemes. Along with these RS selection studies, the optimal deployment of RS should be investigated to improve the efficiency of RSs.

For the optimal RS deployment, the optimal location of the relay station to maximize the system throughput was investigated in [4, 35, 36]. Dong *et al.* evaluated the impacts of variable distances between BS and RS on system capacity through the simulations. They found that when the users are quite close to BS, the two time-slot transmission scheme for relay mode will decrease the capacity, and thus, direct transmission will be better than the two-hop relay transmission. Ge *et al.* developed a non-linear optimization formulation to calculate the optimal RS position. However, the formula does not effectively describe the relationship between capacity and the number of RS. Sadek *et al.* characterized the optimal relay location to minimize the outage probability, and then proposed a nearest-neighbor relay assignment scheme where the nearest neighbor to the source is assigned as a relay station. The above investigations just proposed optimal RS locations in cellular, analyzed the relationship based on simulation results. However, none of them accurately analyzed the problem of “How many relay stations we need to deploy”. In fact, this is very important for the network operators to find a cost-efficient solution of the network deployment.

There exist related works on the RS deployment issue aim to analyze the system capacity enhancement by deploying variable number of RSs [37, 38, 39, 40]. In order to provide interference-free communications, Yang *et al.* presented an orthogonalize-and-

forward relaying scheme [37]. Based on the scheme, a minimum bound on the distributed number of RSs is derived which is 3-5 times of deployed users but it is not realistic for cellular systems or Ad-hoc based one. So *et al.* investigated the optimal utilization of RSs for maximizing system throughput [38]. They evaluated variable number of RSs and distributed location impact on the throughput performance in WLAN. Wang *et al.* proposed an optimal RS deployment solution on cellular environment [39]. They considered the practical cost ratio of BS to RS and their objective was to find the cost-efficient deployment of RSs. Genc *et al.* proposed a max-min fairness based analytical model to analyze the optimal number of RSs [40]. They assumed an IEEE 802.16j based cellular system in the analysis and focused on exploring the effect of number of RSs on the total throughput gain.

However, the optimal number of RSs which are provided in [37, 38, 39, 40] are not valid from the view point of users' QoS requirements. They derived the optimal number of RSs only to maximize the total system performance gains. For example in [40], Genc *et al.* suggested that the system throughput could be maximized when 4 or 5 RSs are located in specific positions where the gain of RSs is maximized. Since they did not consider the QoS requirement of users, however, their scheme cannot guarantee that each user is serviced with application-specific data rate. Furthermore, the analytic models in [38, 39, 40] are applicable only under specific assumptions that RSs and/or users are uniformly distributed in specific positions. Unfortunately, the assumptions are hardly guaranteed in realistic cellular environment where dense buildings and roads are irregularly located.

2.2.2 Analytic Models for Cluster-based Wireless Sensor Networks

LEACH is one of the earliest proposed hierarchical routing protocol that utilizes local CHs operating as routers to the sink node [13]. In addition, it uses an energy efficient clustering scheme that forms nodes into clusters based on received signal strength. Before starting the LEACH algorithm, an initial *CR* value needs to be defined. Then, CHs are

selected according to a threshold value calculated based on the initial CR value. However, the selection of CHs is random, and thus balanced energy consumption among all the nodes is not guaranteed.

A number of methods have been proposed with the aim of solving the drawbacks of LEACH and to further improve network energy efficiency [14, 15, 18]. The closest one is LEACH-E [15], which improves the optimal CR calculation and the cluster formation scheme to balance the energy consumption among CHs. However, the optimal CR values obtained in these methods are confined to clustering with direct transmission, which suffers from high energy-cost required to perform long distance transmissions. In practice, sensor nodes have limited battery power; therefore, the results from the LEACH-based analyses cannot be directly applied to most applications.

Due to the high cost of long distance transmissions, Younis *et al.* proposed the Hybrid, Energy-Efficient and Distributed (HEED) clustering scheme [41], which adopts multi-hop, inter-cluster communication and improves the CH selection scheme of LEACH to balance energy consumption. However, they did not quantitatively analyze the optimal CR value, and instead adopted the optimal CR result from LEACH as their initial CR value and discussed the required CR based on the cluster radius which is a random value. Wei *et al.* aim to relieve the relay load of CHs, which increases as the distance to the sink node decreases [42]. In order to achieve balanced load among CHs, the cluster size is determined based on the distance between a CH and the sink node. Manisekaran *et al.* proposed an energy efficient cluster formation scheme that selects a CH based on data sending rate and redundancy [43]. However, the authors do not provide any mathematical model to analyze the impact of CR on the network performance.

There is only a limited work that mathematically argues the impact of CR on the network performance. Kim *et al.* [44] and Kumar *et al.* [16, 45] show the importance of optimal CR on network performance, and extend the optimal CR analysis in LEACH to multi-hop transmissions using different performance metrics. However, a limitation of

these efforts is that their analyses are performed based on specific energy models, and thus their results cannot be applied to different network environments. Therefore, their analytical models for optimal CR do not reveal the vital relationship between CR and network performance.

Bandyopadhyay *et al.* [46] proposed an analytical model that is derived based on a general energy model. In their work, the optimal CR is obtained by minimizing the network transmission count. However, the approximation applied to their analysis introduces additional calculation errors, and packet retransmission is not considered. Therefore, the optimized CR derived using their analytical model will not efficiently enhance the network lifetime. Ruitao *et al.* [17] proposed an analytical model, which is independent of energy models, to analyze the optimum value for CR . Their analytic model is derived based on the assumption that the network is uniformly divided by clusters. However, this assumption is not generic for most WSN applications, where the location and shape of each cluster are random.

Based on analyzing the features of the existing analytic models discussed above, it is clear that none of these can be efficiently applied in cluster-based WSNs. To fill this gap, this thesis first mathematically analyzes the impact of CR on the network performance. Then, an efficient analytic model is proposed and used to derive the optimal CR value for a generic and feasible network environment where the locations of sensor nodes and clusters are random. In order to allow the analytic model to guarantee network energy efficiency, a joint optimization is performed in terms of inherent transmission count and communication reliability.

Chapter 3

Network Model

This chapter presents the basic assumptions for the considered hierarchical networks. The challenges in developing a feasible analytic model are the analyses complexity and applicability for various network environment. Therefore, this chapter defines a general data propagation model and signal propagation models for the considered hierarchical networks.

3.1 Relay Networks

3.1.1 Relay Model

We consider a cellular environment that has randomly deployed multiple cells in area $A_{cellular}$ and each cell of which the size is A_{cell} contains one BS at its center. Without loss of generality, both RSs and users are distributed by Poisson distribution in each cell and we exploit the nearest-neighbor RS selection scheme [4] which has been proved that it is not only simple but also efficient to set up cooperative pairs. After all of users perform the RS selection process, a cell will be divided into several convex polygons, named clusters, and this process is also well known as Voronoi tessellation [47]. Each cluster consists of an RS at the cluster center and users that are close and thus assigned to the RS. To derive a formula to analyze the impact of the number of RSs on the channel capacity, we make the following assumptions:

- BSs are distributed by Poisson distribution in $A_{cellular}$ with intensity ρ_{bs} , where $A_{cellular}$ is cellular area (When deployed number of BSs is n_{bs} , $\rho_{bs} = n_{bs}/A_{cellular}$).

- There exist some overlapping between BSs' coverage, and the overlap level can be indicated by introducing an overlapping factor $0 < \varepsilon < 1$. Therefore, $A_{cellular} = A_{cell} \cdot n_{bs} \cdot (1 - \varepsilon)$, $\rho_{bs} = (A_{cell} \cdot (1 - \varepsilon))^{-1}$.
- RSs are distributed by Poisson distribution with intensity ρ_{rs} , where $\rho_{rs} = n_{rs}/A_{cell}$. A_{cell} and n_{rs} indicate the cell area and the number of RSs, respectively.
- The number of BSs in the cellular is n_{bs} (i.e., the number of cells, and $n_{bs} = \rho_{bs} \cdot A_{cellular}$) and the overlap level between cells is indicated by overlapping factor ε ($\varepsilon < 1$), thus $A_{cellular} = A_{cell} \cdot n_{bs} \cdot (1 - \varepsilon)$.
- RSs operate according to the time-division model [38]: In the first time-slot, the BS broadcasts a signal to RSs and users, and in the second time-slot, RSs retransmit the received signal to users.
- Users are distributed by Poisson distribution in each cell with intensity ρ_{user} .

3.1.2 Signal Propagation Model

Without loss of generality, the path loss models considered in this thesis is based on IEEE 802.16j standard [48]. In order to simplify the analysis, the path loss models are assumed in suburban environment. In this environment, the path loss covers four categories including type A, B, C, and D. The definitions of the type A, B, C, and D are given in Table 3.1.

Type A, B, and C models are defined for ART (Above Roof Top)-to-BRT (Below Roof Top) environment and type D model is suitable for ART-to-ART. Taking into account the correspondents antenna characteristics, in this thesis, type D is used to evaluate the path loss between BS and RS as shown in Fig. 3.1(a), and type C is used to evaluate the path loss between RS and users as shown in Fig. 3.1(b).

The path loss model for terrain type A/B/C can be derived based on the basic IEEE 802.16 model which is given in the following equation [48].

Table 3.1: Path loss types for IEEE 802.16j based relay networks

| Category | Definition |
|----------|--|
| Type A | ART to BRT for hilly terrain (heavy tree density) |
| Type B | ART to BRT for hilly terrain (moderate tree density) |
| Type C | ART to BRT for flat terrain (light tree densities) |
| Type D | ART to ART |

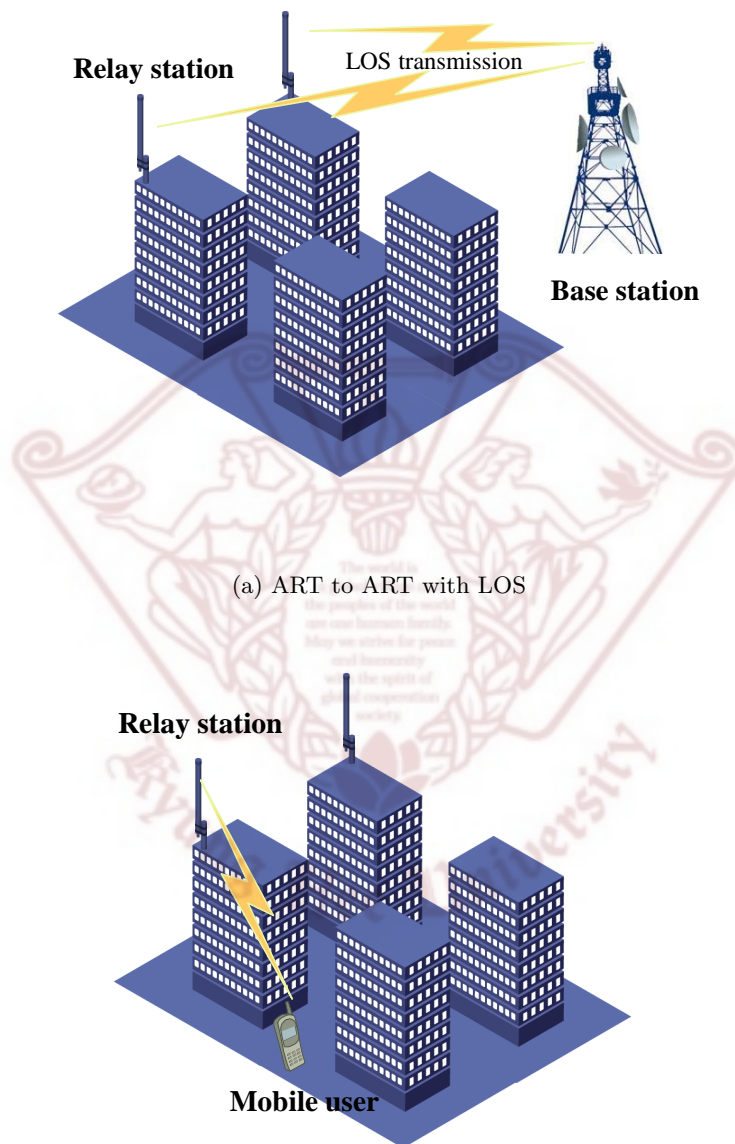
$$PL(d) = \begin{cases} 20 \log \left(\frac{4\pi d}{\omega} \right) & d \leq d'_0 \\ \Gamma + 10 \cdot \gamma \cdot \log_{10}(d/d_0) + \Delta PL_f + \Delta PL_h & d > d'_0 \end{cases}, \quad (3.1)$$

where $d_0 = 100$ m, $d'_0 = d_0 10^{(\Delta PL_f + \Delta PL_h)/(10\gamma)}$ and $d > d_0$. $\Gamma = 20 \cdot \log_{10}(4\pi d_0/\omega)$ and $\gamma = a \cdot b \cdot h_t + c/h_t$. ω (in meter) denotes the wavelength, and h_t is the transmission antenna height and $10 \text{ m} < h_t < 80 \text{ m}$. ΔPL_f is the correction factor for carrier frequency and it is defined as $\Delta PL_f = 6 \cdot \log_{10}(f/2000) \text{ dB}$. ΔPL_h denotes the correction factor for receive antenna height and it is defined as $\Delta PL_h = -10.8 \cdot \log_{10}(h/2) \text{ dB}$. The parameters for different terrain types are given in Table 3.2 [48].

Table 3.2: Parameters for different terrain Type A/B/C

| Parameter | Type A | Type B | Type C |
|-----------|--------|--------|--------|
| a | 4.6 | 4 | 3.6 |
| b | 0.0075 | 0.0065 | 0.005 |
| c | 12.6 | 17.1 | 20 |

As shown in Fig.3.1(a), for the terrain type D, BS and RS antennas are installed above the rooftops and thus they can communicate with LOS (Line of Sight). The path loss model in Type D can refer to Type C because the model is equal to the free space



(b) ART to BRT with LOS or NLOS

Figure 3.1: Signal propagation cases

path loss. Therefore the path loss model of Type D can be defined by Eq. (3.1) and the parameters is the same with Type C.

3.2 Cluster-based Wireless Sensor Networks

3.2.1 Cluster Model

Our cluster model is based on the assumption that sensor nodes are deployed in a network area A using a 2-dimensional Poisson point process with intensity λ . The network contains several clusters and each cluster is managed by a *Cluster Head* (CH). The CHs are selected based on a predetermined CR . In addition to CHs, the other nodes, called *Cluster Members* (CMs), join the CH that is closest to them. The resulting cluster-based network can be regarded as a Voronoi tessellation, where each cluster is a Voronoi cell [49, 47]. Foss *et al.* presented stochastic geometry properties of a Voronoi cell [47]. This thesis models the cluster-based network by extending these properties. In order to achieve this, the following parameters are defined:

- p : Cluster ratio defined as $p = \frac{N_{CH}}{N}$, where N_{CH} and N represent the number of CHs and total number of nodes, respectively.
- λ_{CH} : The density of CH defined as $\lambda_{CH} = \frac{N \times p}{A} = \frac{N_{CH}}{A}$.
- λ_{CM} : The density of CM defined as $\lambda_{CM} = \lambda(1 - p)$
- r : Transmission radius of a node.

3.2.2 Signal Propagation Model

The signal propagation model is based on the *log-normal shadowing path-loss model*, which provides a relatively accurate channel model for WSNs. The path-loss model PL

is represented as

$$PL(d) = PL(d_0) + 10\mu \log_{10} \left(\frac{d}{d_0} \right), \quad (3.2)$$

where d denotes the distance between a sender and a receiver, d_0 is a reference distance, and μ is the path loss exponent. IEEE Std. 802.15.4 specifies a two-segment function for the path-loss model, and defines $\mu = 2.0$ for the first 8 m and then $\mu = 3.3$ for the rest [50]. Therefore, the path-loss model of IEEE Std 802.15.4 is represented as

$$PL(d) = \begin{cases} PL(d_0) + 10\mu \log_{10}(d) & d \leq d'_0 \\ PL(d'_0) + 10\mu \log_{10} \left(\frac{d}{d'_0} \right) & d > d'_0 \end{cases}, \quad (3.3)$$

where $d_0 = 1$ m, $d'_0 = 8$ m, $\mu = 2$ if $d \leq d'_0$, and $\mu = 3.3$ if $d > d'_0$. The path loss at the reference distance (d_0) is given by

$$PL(d_0) = 10\mu \log_{10} \left(\frac{4\pi d_0 f}{C} \right), \quad (3.4)$$

where f is the signal frequency and C is the speed of light.

3.2.3 Data Propagation Model

This thesis classifies intra- and inter-cluster data propagation as either direct or multi-hop. Fig. 3.2 shows the three data propagation models in cluster-based WSNs. CMs transmit sensed data to their CH either directly or using multi-hop, which is also the case for communications between CHs and the sink node. Fig. 3.2(a) shows the *single-hop to single-hop* (*s2s*) case, where data propagation within intra-cluster and inter-cluster is performed using direct transmission. Prior research has shown that when the network range is wide, the energy consumption for *s2s* data transmission is excessive, and thus not applicable in most WSN applications. Therefore, this data propagation model is not considered in our analysis. Fig. 3.2(b) shows the *multi-hop to multi-hop* (*m2m*) case, where data propagation is performed using multi-hop transmission with short intra-cluster and inter-cluster communications. Finally, Fig. 3.2(c) shows the *multi-hop to single-hop*

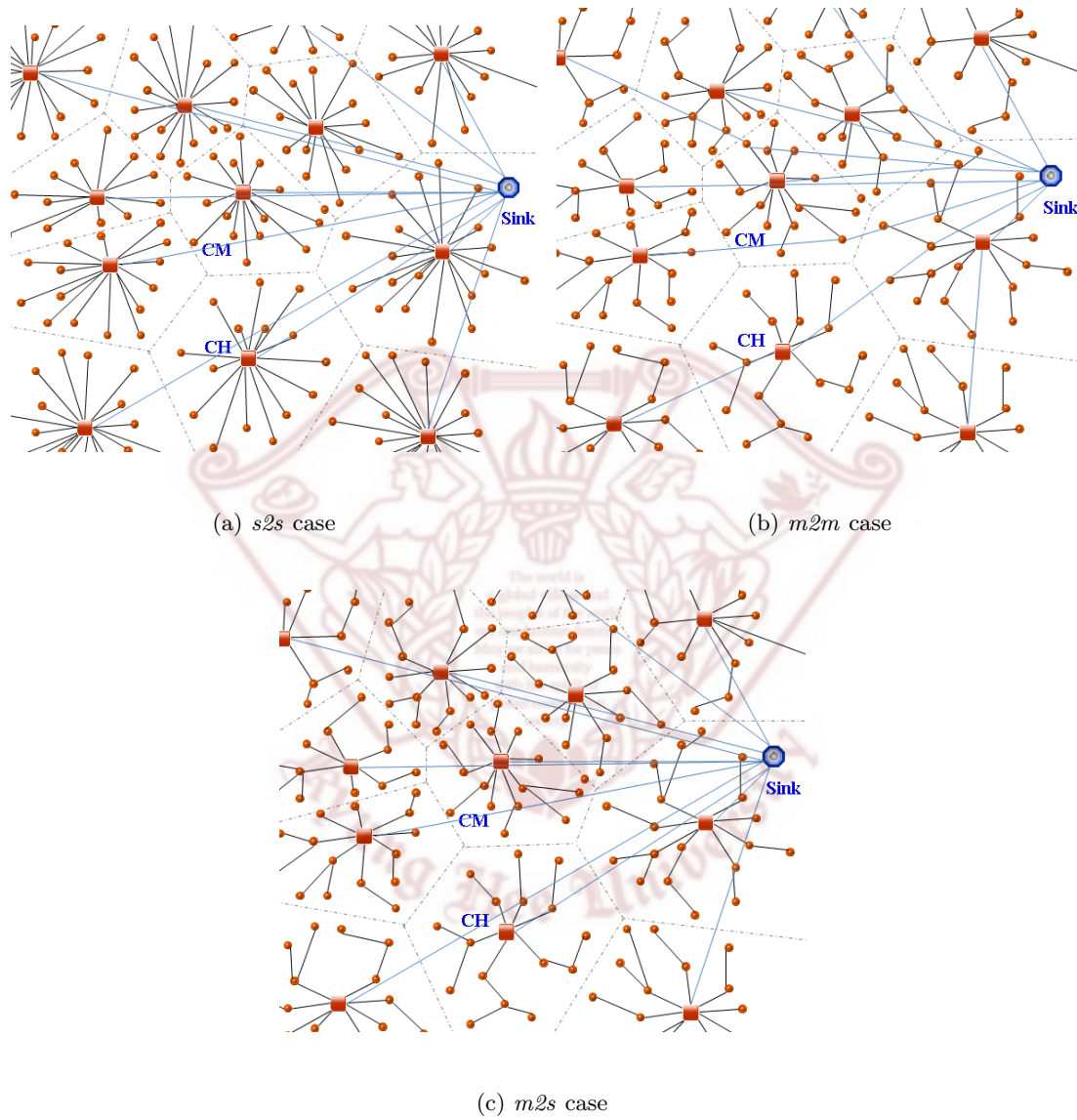


Figure 3.2: Data propagation models

(*m2s*) case, which reduces the energy consumed by the nodes that are near to the sink node by employing long-range, low-power RF module (such as low-power Bluetooth) to support direct transmission between CHs and the sink node. Therefore, data propagation

is performed using multi-hop transmission with short intra-cluster communications and direct transmission with long distance inter-cluster communications.



Chapter 4

Analytic Model for Optimizing Cost Efficiency in Relay Networks

The RS (Relay Station) has become an important radio resource in next generation wireless communication systems. The optimal number of RSs is one of the crucial issues in configuring a cost-effective RS-based network architecture. In this chapter, we present a practical analytic model to describe the impact of the number of RSs on the channel capacity of two-hop relay network. From the mathematical analysis, the optimal number of RSs is obtained to satisfy QoS requirements of users considering various levels of MCS (Modulation and Coding Scheme). In addition to the mathematical analysis to determine the feasibility of the analytic model, we also examine its performance through a set of simulations. The simulation results show the validity of the proposed analytic model.

4.1 Overview

Cooperative communications have been adopted as a promising solution to achieve high data rates by minimizing the signal fading problem. The basic idea of relay networks is that multiple RSs are distributed in a cell and each RS with a single antenna can cooperate with others by composing virtual antenna arrays in order to confer benefits similar to those provided by conventional MIMO (Multiple-Input Multiple-Output) systems.

These benefits are significant, and thus, a significant amount of research has been devoted to efficiently use radio resources of RSs. There are two main problem for effi-

ciently utilizing the RSs which are "Where to deploy RSs", and "How many RSs should be deployed". The first problem is addressed for determining the optimal location for improving the network performance in terms of system throughput and coverage extension [38, 39]. However, it is hard to develop an public analytic model because the analyses are closely correlated with the network terrain and the specific network configuration. The other issue is interested by the network operator because it is important for minimizing the network investments and operating costs.

In the following Sec. 4.2, we propose an analytic model for the optimal number of RSs that can satisfy users' QoS requirements based on a general assumption that RSs and users are randomly distributed by Poisson point process. In order to achieve this, we mathematically analyze the stochastic geometry of network and the impact of the number of RSs on the average channel capacity. In order to guarantee the QoS requirement, the AMC (Adaptive Modulation and Coding) scheme is taken into account in the proposed analytic model. Consequently, the proposed model derives not only the lower bound on the number of RSs but also the optimal number of RSs for various levels of MCS (Modulation and Coding Scheme).

4.2 Analysis on the Optimal Network Structure

In order to mathematically analyze the impact of the number of RSs on the network performance, Sec. 4.2.1 analyzes the stochastic geometry in the RS served region first. Then, Sec. 4.2.2 mathematically evaluates the average channel capacity of RS. Finally, Sec. 4.2.3 derives the analytic model for optimizing the number of RSs.

4.2.1 Analysis on Stochastic Geometry in the Relay Station Served Region

According to the basic assumptions in Sec. 3.1.1. a relay station served region is a convex polygon named as the Voronoi cell, and all the cells of the network create Voronoi tessellation [47]. Based on that, applying the properties of Palm distribution [49], the first moment of aggregate characteristics can be given as below, where $f(x)$ is a non-negative function.

$$E(S_f) = \rho_{user} \int f(x) e^{-\rho_{rs}\pi|x|^2} dx \quad (4.1)$$

First, we reduce the complexity of analysis in cluster domain. By taking $f(x) = 1$ and $f(x) = l$ (where l is the link length between correspondents), we can determine the expectations of the number of users (N_{user}) and the total link length (L_t) of users connected to the RS in a cluster as shown in Eqs. (4.2) and (4.3), respectively:

$$E(N_{user}) = \frac{\rho_{user}}{\rho_{rs}} \quad (4.2)$$

$$E(L_t) = \frac{\rho_{user}}{2\rho_{rs}^{3/2}} \quad (4.3)$$

According to Eqs. (4.2) and (4.3), which are derived from the Voronoi tessellation, the average link length of each cluster can be expressed as follows:

$$E(L_{avg.}) = \frac{E(L_t)}{E(N_{user})} = \frac{1}{2\sqrt{\rho_{rs}}} \quad (4.4)$$

When we substitute $\rho_{rs} = n_{rs}/A_{cell}$ into $E(L_{avg.})$ in Eq. (4.4), $E(L_{avg.})$ can be expressed as follows:

$$E(L_{avg.}) = \sqrt{\frac{A_{cell}}{4n_{rs}}} \quad (4.5)$$

In generally, a cellular system coverage ($A_{cellular}$) consist with several sub-coverage of A_{cell} and there are some overlaps between A_{cell} (result in $A_{cellular} \leq n_{bs} * A_{cell}$). Consequently, the relation between the intensity of BS (ρ_{bs}) and the coverage area provided

by the BS can be indicated by the following inequality. By introducing the overlapping factor ε into Eq. (4.6), we can get $\rho_{bs} = (A_{cell} * (1 - \varepsilon))^{-1}$.

$$\begin{cases} \rho_{bs} * A_{cellular} * A_{cell} \geq A_{cellular} \\ A_{cell} > 0 \\ A_{cellular} > 0 \end{cases} \Rightarrow \rho_{bs} \geq \frac{1}{A_{cell}} \quad (4.6)$$

In the same way in which we derived Eq. (4.3), the expected total and average link length between BS and RSs can be derived as shown in Eqs. (4.7) and (4.8), respectively.

$$E(L_{bs2rs}) = \frac{n_{rs}/A_{cell}}{2(1/(A_{cell} \cdot (1 - \varepsilon)))^{3/2}} \quad (4.7)$$

$$E(L_{bs2rs}^{avg.}) = \frac{E(L_{bs2rs})}{n_{rs}} = \frac{(1 - \varepsilon)^{3/2} \cdot \sqrt{A_{cell}}}{2} \quad (4.8)$$

4.2.2 Evaluating Channel Capacity of Relay Stations

Based on Shannon capacity theory, one-hop channel capacity can be calculated by using Eq. (4.9) and the equation indicates that the channel capacity (C) is a function of SNR (Signal-to-Noise Ratio) and channel bandwidth (B).

$$C = B \log_2(1 + SNR) \quad (4.9)$$

In order to analyze the relation between the number of RSs and the channel capacity, we need to modify Eq. (4.9). First, P_{tx} and P_{rx} are defined as the lower bounds of the transmit power and receive power, respectively. Simultaneously, P_{tx} and P_{rx} can be expressed as $P_{tx} = P_{rx} - G_{tx} - G_{rx} + P_L + M_{Fade}$ and $P_{rx} = N_{RNF} + SNR$, respectively (N_{RNF} means receiver noise floor). To simplify the equation, the system parameters are defined as $\alpha = P_{tx} + G_{tx} + G_{rx} - M_{Fade} - N_{RNF}$ and SNR can be expressed as shown below: (The parameters used in this Sec. are defined in Table 4.1.)

$$SNR = \alpha - P_L \quad (4.10)$$

Table 4.1: Parameter notation and definition

| Parameter | Definiton |
|--|---|
| B | Channel bandwidth 10 MHz |
| $G_{tx} G_{rx}$ | tx and rx antenna gain(18, 0) dBi |
| M_{Fade} | Fade margin 19.56 dB |
| N_{RNF} | Thermal noise + Noise figure + 10 log B |
| f | Frequency 3500 Mhz |
| h_{bs}, h_{rs}, h_{user} | BS, RS and user antenna ht.(80, 10, 1.7) m |
| Γ, d_0 | $\Gamma = 20 \cdot \log_{10}(4\pi d_0/\lambda)$, $d_0 = 100$ m |
| γ | $\gamma = a \cdot b \cdot h_t + c/h_t$ |
| h_t | Transmission antenna height (h_{bs}, h_{rs}) |
| Type C, D (a, b, c) | 3.6, 0.005, 20 |
| $\Delta PL_f, \Delta PL_h$ | $\Delta PL_f = 6 \cdot \log_{10}(f/2000)$ dB, |
| (Type C, D) | $\Delta PL_h = -10.8 \cdot \log_{10}(h/2)$ dB |
| ε | 0.15 |
| MAPL(16QAM 1/2, QPSK 1/2, QPSK 1/8) | 128.2 dB, 133.7 dB, 136.4 dB |

Next, we determine the path loss model (P_L) in Eq. (4.10). There exist a lot of path loss models for various radio propagation environments. As mentioned in Sec. 3.1.2, we derive a mathematical analysis based on the Erceg path loss model which is recommended in IEEE 802.16 standard. The other propagation models, however, can be applied to our

analysis. P_L is defined by the following equation [51, 48].

$$P_L = \Gamma + 10 \cdot \gamma \cdot \log_{10}(d/d_0) + \Delta PL_f + \Delta PL_h \quad (4.11)$$

Finally, when $\beta = 1 - \Gamma - \Delta PL_f - \Delta PL_h$, Eq. (4.9) can be changed to a function of d which denotes the distance between correspondents as the following formula and we define $f(d) = B \log_2(\alpha + \beta - 10 \cdot \gamma \cdot \log_{10}(d/d_0))$.

$$C = f(d) \quad (4.12)$$

4.2.3 Analytic Model for Optimizing the Number of Relay Stations

According to the investigation in [52], the end-to-end two-hop channel capacity (C_{e2e}) is expressed as shown in Eq. (4.13). In Eq. (4.13), C_{bs2rs} , $C_{rs2user}$, D_{bs2rs} , and $D_{rs2user}$ denote one-hop channel capacity and the distance between the correspondents.

$$C_{e2e} = \left(\frac{1}{C_{bs2rs}} + \frac{1}{C_{rs2user}} \right)^{-1} = \frac{C_{bs2rs} \cdot C_{rs2user}}{C_{bs2rs} + C_{rs2user}} \quad (4.13)$$

We substitute $C_{bs2rs} = f(D_{bs2rs})$ and $C_{rs2user} = f(D_{rs2user})$ in Eq. (4.13), which yields Eq. (4.14) as follows:

$$C_{e2e} = \frac{f(D_{bs2rs}) \cdot f(D_{rs2user})}{f(D_{bs2rs}) + f(D_{rs2user})} \quad (4.14)$$

Next, if we substitute $E(L_{avg.})$ and $E(L_{bs2rs}^{avg.})$ in Eqs. (4.6) and (4.8) for $D_{rs2user}$ and D_{bs2rs} , the relation between the two-hop channel capacity and the number of RSs is clarified in Eq. (4.15). The equation describes the distance between BS and RS and the number of RSs which impacts on the channel capacity. In this thesis, we use Eq. (4.15) to analyze the lower bound on the number of RSs, and then we obtain the optimal number of RSs for various levels of MCS.

$$C_{e2e} = \frac{f\left(\frac{(1-\varepsilon)^{3/2} \cdot \sqrt{A_{cell}}}{2}\right) \cdot f\left(\sqrt{\frac{A_{cell}}{4n_{rs}}}\right)}{f\left(\frac{(1-\varepsilon)^{3/2} \cdot \sqrt{A_{cell}}}{2}\right) + f\left(\sqrt{\frac{A_{cell}}{4n_{rs}}}\right)} \quad (4.15)$$

4.3 Performance Evaluation

The Erceg path loss model covers four categories including type A, B, C, and D [51]. Type A, B, and C models are suitable for ART (Above Roof Top)-to-BRT (Below Roof Top) environment and type D model is suitable for ART-to-ART. Taking into account the correspondents' antenna characteristics, type D is used to evaluate the path loss between BS and RS and type C is used to evaluate the path loss between RS and users. Type C and D path loss models are defined in Eq. (4.11) and the values of parameters are listed in Table 4.1. The total bandwidth is 10 MHz and the power available at both BS and RS is 43 dBm , while we neglect shadow fading and multi path fading in the simulation. BS provides the cell coverage with a radius of 3.2 km and both RSs and users are randomly distributed in a cell coverage area. More detailed simulation parameters are shown in Table 4.1.

Based on these simulation parameters, Sec. 4.3.1 evaluate the accuracy of the analytic model through comparing the approximation results with simulation. Furthermore, Sec. 4.3.2, confirms the performance of the proposed analytic model.

4.3.1 Validation of the Approximation Efficiency

In Fig. 4.1, the numerical results obtained from Eq. (4.15) are compared with the simulation results of two-hop channel capacity. The graph shows that the simulation results are very close to the numerical one based on Eq. (4.15). The comparison indicates that our proposed analytic model can reflect the impact of the number of RSs on the average link length in a cluster and express the channel capacity between the users and RSs. Through our mathematical analysis of which the accuracy is proved in Fig. 4.1, we can predict the system channel capacity under the given number of RSs.

In addition, by comparing the channel capacity with the direct transmission, the intersection in Fig. 4.1 indicates a lower bound on the number of RSs which should

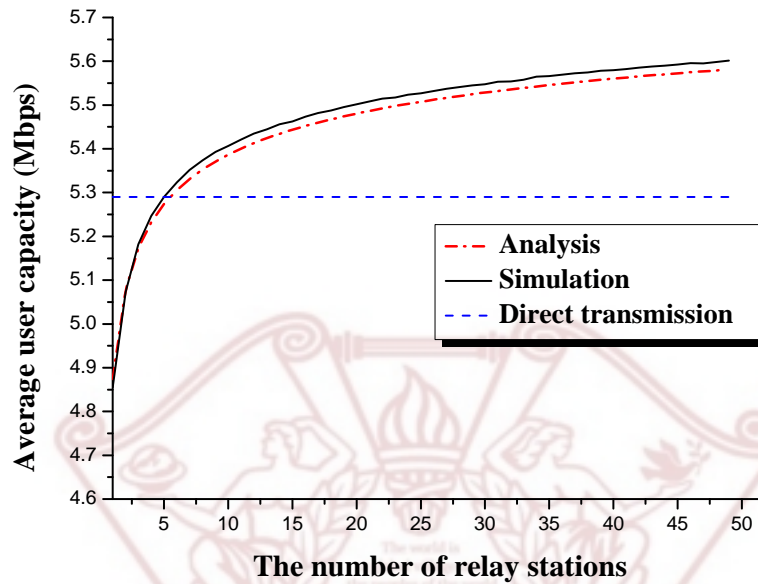


Figure 4.1: Numerical analysis and simulation results

be distributed. At the left side of the intersection, we can find that direct transmission outperforms two-hop relay transmission. This is because the capacity gain obtained by RSs is smaller than one which is decreased by two time-slot transmission. When more than six RSs are deployed, however, the average channel capacity is improved as shown in Fig. 4.1.

4.3.2 Performance of the Proposed Analytic Model

Next, Fig. 4.2 shows the average path loss analysis in a cluster assuming that RSs provide services with QPSK 1/8, QPSK 1/2, and 16-QAM 1/2 MCS and the MAPL (Maximum Allowable Path Loss) in a cluster is given 136.4 dB, 133.7 dB, and 128.2 dB for each MCS level [53]. From the analysis results shown in Fig. 4.2, we obtain the optimal number of RSs to the MAPL requirement of MCS where it is 13, 16, and 27, respectively. It can

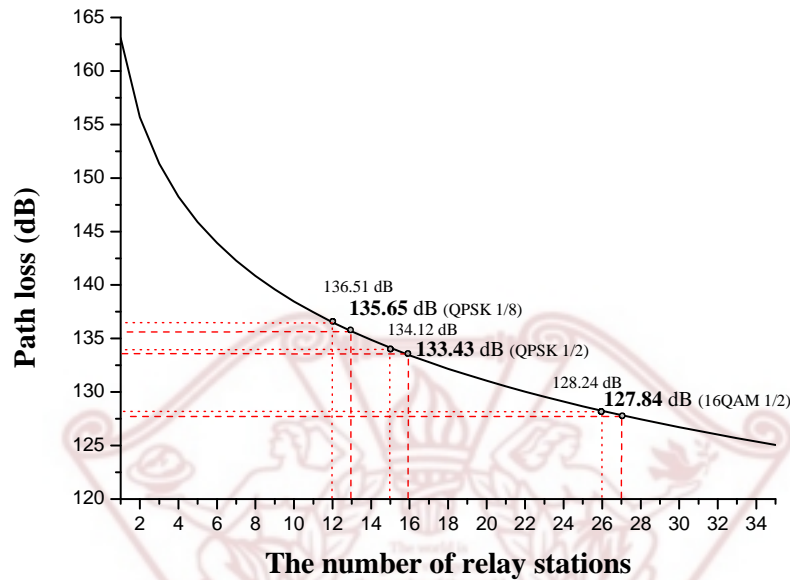


Figure 4.2: Average path loss analysis in a cluster

be observed that the optimal number of RSs can effectively guarantee various users' QoS requirements in Fig. 4.2.

Fig. 4.3 shows spectral efficiency by deploying different optimal number of RSs. In the simulation, when AMC scheme is adopted in RSs, the RSs adaptively select suitable MCS after evaluating current channel state (i.e., SNR). With the iteration over 1500, it can be observed that average spectral efficiency converge into 1.5 bps/Hz , 1.14 bps/Hz and 0.95 bps/Hz , respectively. The spectral efficiency approximately reaches the standard spectral efficiencies which are provided by different MCSs i.e., 1.6 bps/Hz (16-QAM 1/2), 0.81 bps/Hz (QPSK 1/2) and 0.2 bps/Hz (QPSK 1/8). The observation indicates the proposed optimal number of RSs can efficiently guarantee target MCS in the network. Users' requirement of transmission rate can also be guaranteed because every user in the system should be supported by their expected MCS with high-probability.

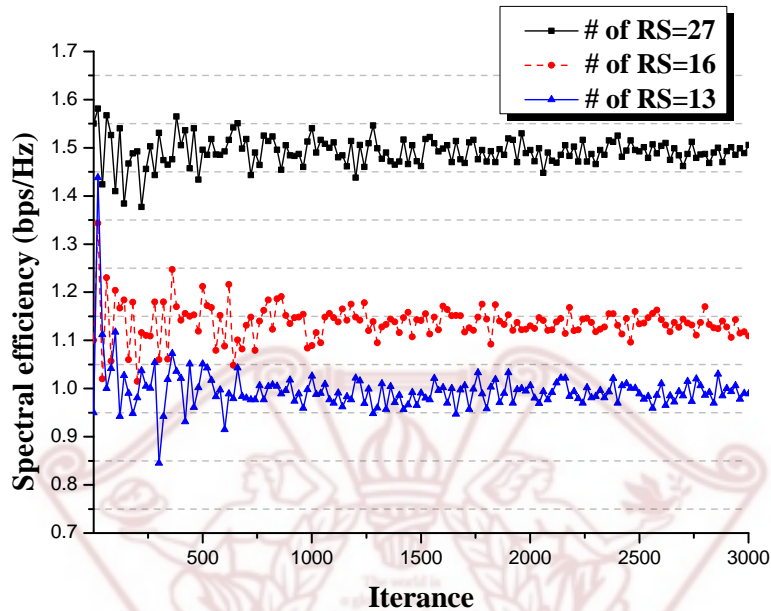


Figure 4.3: Spectral efficiency with different number of RSs

Consequently, when an expected QoS requirement is given in network planning point of view, the proposed analytic model can provide not only the lower bound on the number of distributed RSs but also the optimal number of RSs for various levels of MCS to guarantee the QoS requirements.

4.4 Summary

Relay networks introduced a novel radio resource RS for next generation wireless communication and the proper number of RSs should be deployed to enhance the channel capacity. In this chapter, we analyzed the impact of the number of RSs on the average link length between user and RS, and then derived an analytic model to determine the lower bound on the number of distributed RSs and the optimal number of RSs for various

levels of MCS. The proposed analytic model was validated through a set of simulations. When we consider both cost-effectiveness and users' QoS requirement at the same time, our analytic model can provide an effective solution on the optimal number of RSs.



Chapter 5

Analytic Model for Optimizing Energy Efficiency in Cluster- based Wireless Sensor Networks

In wireless sensor networks, clustering schemes have been adopted as an efficient solution to prolong the network lifetime. In these schemes, the performance of energy-efficient data transmission is affected the cluster ratio. This chapter analyzes the optimal cluster ratio from the perspective of network energy efficiency, and its impact on the network lifetime. In order to provide a practical analytic model, various data propagation cases are mathematically analyzed. In addition, the network lifetime is extended by jointly optimizing the network transmission count and link reliability.

5.1 Overview

A Wireless Sensor Network (WSN) is a multi-hop based network that allows sensor devices to communicate without any network infrastructure. It consists of a large number of tiny sensor nodes each equipped with a microprocessor, a memory, sensing modules, radio transceivers, and a battery. WSNs are widely deployed in environment monitoring, health-care, intrusion detection, etc., and play a key role in the Internet of Things (IoT) paradigm. However, sensor nodes have limited battery power, and therefore, energy efficiency is crucial for prolonging the network lifetime of WSNs.

In order to prolong the network lifetime, many schemes have been proposed with energy efficiency in mind, such as energy efficient Media Access Control (MAC) and routing schemes. Furthermore, some research efforts have been made on exploring energy efficient network architectures. For example, Heinzelman *et al.* proposed a cluster-based communication protocol called Low-Energy Adaptive Clustering Hierarchy (LEACH) [13], which is the most well-known clustering scheme for WSNs. Recently, clustering schemes have been explored to enhance energy efficiency and communication performance, as well as improve network scalability [7, 8, 9, 10, 11]. Clustering schemes in WSNs can decrease the amount of transmitted traffic at a Cluster Head (CH) using data aggregation, and thus energy can be saved during data transmission [12]. In addition, since nodes are managed as a cluster, the network becomes more robust and the overhead due to frequent topology changes is reduced.

Existing works [13, 14, 15, 17, 16, 18, 45, 46], indicate that an improper choice of Cluster Ratio CR will result in extra energy dissipation, and thus an appropriate choice of CR is critical for enhancing the network lifetime. For this reason, a practical analytic model is desired for optimizing the CR to prolong the network network life time. For the cluster-based WSN, this thesis analyzes the relationship between Cluster Ratio CR and network performance for improving the network energy efficiency. This is achieved by modeling a cluster-based WSN as a 2-dimensional Poisson point process and analyzing the impact of CR on the network performance in terms of transmission count and *Packet Reception Ratio* (PRR). Then, a joint optimization scheme is proposed to derive the optimized CR that guarantees network energy efficiency and prolongs network lifetime.

5.2 Analysis on the Optimal Network Structure

In a sensor device, energy is mainly consumed by the computational component and the RF module. Akyildiz *et al.* showed that the energy consumption of the RF module

is 10 times that of the computational component [7, 24]. Therefore, energy efficiency in WSNs is mainly constrained by the number of wireless communications consisting of both transmissions and retransmissions. For this reason, our objective is to improve the network energy efficiency by minimizing the number of inherent transmissions and retransmissions.

Sec. 5.2.1 mathematically analyzes the impact of CR on the inherent transmission count of a network. Sec. 5.2.2 explores the impact of CR on Packet Reception Ratio (PRR) to maximize communication reliability. Finally, Sec. 5.2.3 presents a joint optimization scheme to derive the optimal CR , which simultaneously optimizes both the inherent transmission count and the communication reliability, i.e., PRR .

5.2.1 Optimal Cluster Ratio for Minimizing Inherent Transmission Count

In this thesis, WSN is employed to monitoring a large scale area, and a densely deployed network is assumed in which the sensor nodes' connectivity can be guaranteed. This is a fair assumption because the node density in the considered sensor network applications in the large scale area ¹ tends to be higher than the minimum node density requirement², which is just enough to guarantee the network connectivity to provide network redundancy and to make sure that a point in a region of interest can be sensed by more than one sensor node [54, 55, 56]. Furthermore, in order to analyze and quantify the transmission count in cluster-based WSNs, the following definition is provided for the *Inherent Transmission Count (ITC)*:

Definition 5.2.1. *Inherent Transmission Count (ITC) represents the total number of*

¹Applications such as environmental monitoring, battle field and border surveillance are assumed in this thesis.

²Lower bound of the deployed node density should be efficient to guarantee that there are no isolate sensor nodes, which means isolate probability of a sensor node in the network should be equal to 0 (The relation between isolate probability and node density will be given in Sec. 5.2.2).

transmissions in a cluster-based WSN when all the nodes send a packet to the sink node according to a predetermined transmission strategy.

ITC is composed of intra-cluster and inter-cluster transmission counts. The following theorem characterizes the relationship between *CR* and *ITC*:

Theorem 5.2.1. *For a given routing strategy and a clustering scheme in a cluster-based WSN, *ITC* is a convex function of *CR* for the *m2s* and *m2m* data propagation cases.*

Proof. The data propagation models *m2s* and *m2m* employ multi-hop transmission within a cluster. Therefore, the expected number of transmissions within a cluster needs to be first analyzed.

As stated in Sec. 3.2.1, a cluster can be regarded as a Voronoi cell [47, 49]. Foss *et al.* [47] analyzed the geometrical properties of a Voronoi cell (i.e., a cluster) in polar coordinates, and assumed that a CH is in 0 point. One of the important results they obtained is the expected number of nodes in a Voronoi cell, $E[N_{tot}]$, which is given as (See [47] for a complete proof of Eq. (5.1))

$$\begin{aligned} E[N_{tot}] &= \lambda_{CM} 2\pi \int_0^\infty l e^{-\lambda_{CH} \pi l^2} dl, \\ &= \frac{\lambda_{CM}}{\lambda_{CH}}, \end{aligned} \quad (5.1)$$

where l denotes the radius of a cluster. In Eq. (5.1), $E[N_{tot}]$ is derived by integrating $2\pi l \lambda_{CM} e^{-\lambda_{CH} \pi l^2} dl$, where $2\pi l dl$ is the area element and $e^{-\lambda_{CH} \pi l^2}$ is the probability of a node belongs to the CH.

The same method is applicable for calculating the number of nodes located in the i -th hop. For the analysis, the integration interval $(0, \infty+)$ can be subdivided into the minimum transmission range of CM, r_{min} . Therefore, a cluster can be regarded as dividing it into k ($k \rightarrow \infty+$) doughnut-shaped regions where each region has a width equal to r_{min} . Let $E[N_{CM}^i]$ represent the number of nodes in the i -th doughnut. Based

on Eq. (5.1), $E[N_{CM}^i]$ can be derived as

$$\begin{aligned} E[N_{CM}^i] &= \lambda_{CM} 2\pi \int_{(i-1)r_{min}}^{ir_{min}} l e^{-\lambda_{CH}\pi l^2} dl, \\ &= \frac{\lambda_{CM}}{\lambda_{CH}} \left(e^{-\lambda_{CH}\pi((i-1)r_{min})^2} - e^{-\lambda_{CH}\pi(ir_{min})^2} \right). \end{aligned} \quad (5.2)$$

Eq. (5.2) satisfies $\sum_{i=1}^k E[N_{CM}^i] = E[N_{tot}]$ when $k \rightarrow \infty+$, and the complete proof of Eq. (5.2) is given in the Appendix A. In addition, simulation results that validate the approximation efficiency of Eq. (5.2) are presented in Sec. 5.3.1. Since the sensor nodes are assumed to be densely deployed, the transmission hop-count of the node in the i -th doughnut can be approximated by i hops, and the expected total transmission count of the i -th doughnut is represented as $i \cdot E[N_{CM}^i]$. The total transmission count in a cluster $E[H]$ is a cumulative function of i from 0 to k given by the following equation:

$$\begin{aligned} E[H] &= \sum_{i=1}^k i E[N_{CM}^i] \\ &= \frac{\lambda_{CM}}{\lambda_{CH}} \left(1 + \sum_{i=1}^k e^{-\lambda_{CH}\pi(ir_{min})^2} \right) \\ &= \frac{\lambda_{CM}}{\lambda_{CH}} \sum_{i=0}^k e^{-\lambda_{CH}\pi(ir_{min})^2}. \end{aligned} \quad (5.3)$$

There are $N \cdot p$ clusters in the network; therefore the total expected transmission count $E[H_{tot}] = NpE[H]$, and it is given by

$$E[H_{tot}] = Np \frac{\lambda_{CM}}{\lambda_{CH}} \sum_{i=0}^k e^{-\lambda_{CH}\pi(ir_{min})^2}, \quad (5.4)$$

where $k \rightarrow \infty$. However, the time calculation for $k \rightarrow \infty+$ is time consuming and not necessary because $\lim_{k \rightarrow \infty+} e^{-\lambda_{CH}\pi(kr_{min})^2} = 0$, which means that when $k \rightarrow \infty$ the node is more likely to be within the range of other CHs. In actuality, if a node is not within the range of a cluster, l , the probability $e^{-\lambda_{CH}\pi(ir_{min})^2} \rightarrow 0$. Therefore, k in Eq. (5.4) can be approximated by $\lceil l/r_{min} \rceil$. Note that both the shape and radius of a cluster is random; therefore, the average radius of a cluster l is also a random value. In order to obtain the

expected radius of a cluster, $E[l]$, the result from [47] is utilized, which showed that the total direct link length of a cluster is $E[L_{tot}] = \lambda_{CM}/2\lambda_{CH}^{3/2}$. After obtaining $E[L_{tot}]$ and $E[N_{tot}]$, $E[l]$ can be derived as follows:

$$E[l] = \frac{E[L_{tot}]}{E[N_{tot}]} = \frac{1}{\sqrt{4\lambda_{CH}}} = \sqrt{\frac{A}{4Np}}. \quad (5.5)$$

Since $k = \lceil E(l)/r_{min} \rceil = \lceil \sqrt{\frac{A}{4Nr_{min}^2 p}} \rceil$, substituting $\lambda(1-p)$ for λ_{CM} and $\frac{(1-p)}{p}$ for $\frac{\lambda_{CM}}{\lambda_{CH}}$ into Eq. (5.4) yields the total transmission count in $N \cdot p$ clusters, $E[H_{tot}(p)]$, given as

$$E[H_{tot}(p)] = N(1-p) \sum_{i=0}^{\lceil \sqrt{\frac{A}{4Nr_{min}^2 p}} \rceil} e^{-\lambda p \pi (ir_{min})^2}. \quad (5.6)$$

Next, the *ITC* between CHs and the sink node is analyzed. For the *m2s* case, the total transmission count $E[H'_{tot}]$ is equal to the number of CHs because they directly transmit both the generated and received data to the sink node. Thus, the expected *ITC* for the *m2s* case, $E[ITC_{m2s}(p)]$, is given as

$$E[ITC_{m2s}(p)] = N(1-p) \sum_{i=0}^{\lceil \sqrt{\frac{A}{4Nr_{min}^2 p}} \rceil} e^{-\lambda p \pi (ir_{min})^2} + Np. \quad (5.7)$$

For the *m2m* case, CHs transmit packets to the sink node using multi-hop; therefore, the *ITC* between CHs and the sink node can be derived using the same method for the intra-cluster case. However, the densities of CMs and CHs need to be replaced by the density of CHs and the sink node, which are denoted by $\lambda'_{CH} = \lambda p$ and $\lambda_{sink} = \frac{1}{A}$, respectively. Based on Eq. (5.2), the transmission count between CHs and the sink node, $E[H_{tot}(p)']$, is given by

$$\begin{aligned} E[H_{tot}(p)'] &= \frac{\lambda'_{CH}}{\lambda_{sink}} \sum_{i=0}^{\lceil \frac{R}{r} \rceil} e^{-1/A\pi(ir)^2} \\ &= Np \sum_{i=0}^{\lceil \frac{R}{r} \rceil} e^{-1/A\pi(ir)^2}, \end{aligned} \quad (5.8)$$

where r and R denote the transmission range of CH and the network radius, respectively. Based on this, the expected ITC for the $m2m$ case, $E[ITC_{m2m}(p)]$, can be derived as

$$E[ITC_{m2m}(p)] = N(1-p) \sum_{i=0}^{\lceil \sqrt{\frac{A}{4Nr_{min}^2 p}} \rceil} e^{-\lambda p \pi (ir_{min})^2} + Np \sum_{i=0}^{\lceil \frac{R}{r} \rceil} e^{-1/A\pi(ir)^2}. \quad (5.9)$$

Therefore, ITC for both $m2s$ and $m2m$ cases can be determined based on the cluster ratio p and the static network parameters, i.e., node density λ , network area A , and transmission ranges r and r_{min} .

The convexity of Eqs. (5.7) and (5.9) can be proved by second-order conditions. In Eq. (5.7), the terms $N(1-p)$ (when $i=0$) and Np are linear functions, which have both concave and convex properties. Let $f(p) = e^{-\lambda p \pi (ir_{min})^2}$ for $0 < i \leq \lceil \sqrt{\frac{A}{4Nr_{min}^2 p}} \rceil$, then the second-order of $f(p)$ is given by the following equation:

$$f''(p) = (1-p)N(\lambda \pi r_{min}^2 i^2)^2 e^{-\lambda p \pi (ir_{min})^2} + 2N\lambda \pi r_{min}^2 i^2 e^{-\lambda p \pi (ir_{min})^2}, \quad (5.10)$$

where $0 < p < 1$. Eq. (5.10) shows that the condition $f''(p) > 0$ is always satisfied for any value of i ; therefore, $f(p)$ is a convex function for $0 < p < 1$.

Based on the above results, Eq. (5.7) is a nonnegative weighted sum of convex functions that preserves convexity of functions; therefore, it can be proved that it is a convex function. The convexity of Eq. (5.9) can be proved in a similar fashion, and thus the proof is complete. □

Theorem 5.2.1 shows an important relationship between cluster ratio p and ITC , and it indicates that there exists an optimized p to minimize ITC . Fig. 5.1(a) and Fig. 5.1(b) show the ITC values as a function of p for the $m2s$ and $m2m$ cases, respectively.

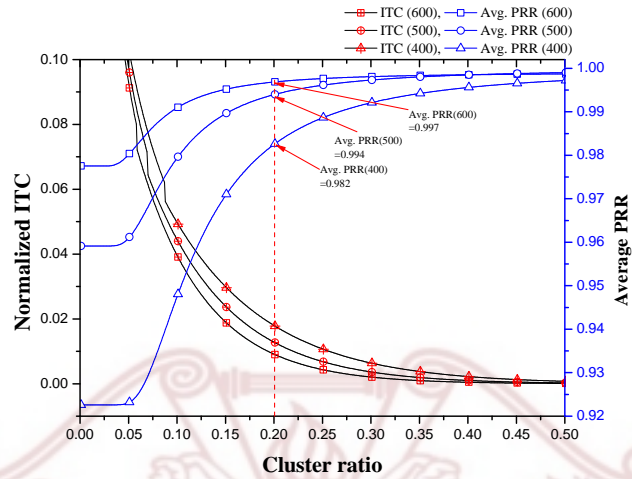
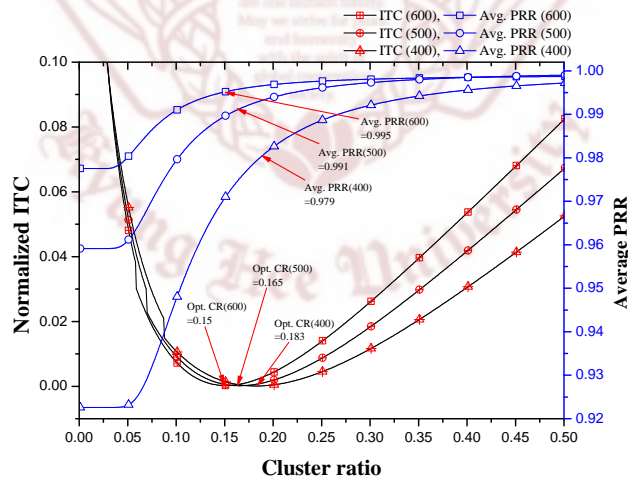
(a) *m2s* case(b) *m2m* case

Figure 5.1: The impact of Cluster Ratio on normalized *ITC* and *PRR* ($k = 3.3$ and $r_{min} = 10$ m)

The results in these figures show that for the $m2m$ case, Eq. (5.9) is strictly convex, and there is only one optimum solution for p . However, for the $m2s$ case, Eq. (5.7) is not a strictly convex function; therefore, an additional restricted condition is needed to determine an appropriate p .

5.2.2 Optimal Cluster Ratio for Maximizing Communication Reliability

The optimum p for ITC does not necessarily guarantee energy efficiency because packet retransmissions will decrease the performance of the optimized solutions. Therefore, this subsection explores an energy efficient solution from the perspective of communication reliability, and analyzes the trade-off between minimizing ITC and maximizing PRR in cluster-based WSNs.

Given a network, let \mathbb{P} indicate a Bernoulli random value. If a packet is successfully received, $\mathbb{P} = 1$; otherwise, $\mathbb{P} = 0$. Assuming \mathbb{P} is independent and identically distributed (iid) and according to the weak law of large numbers, PRR can be statistically approximated by the following equation:

$$\mathbb{P} = PRR = (1 - \mathbb{P}_b)^{8F}, \quad (5.11)$$

where F indicates frame size in bytes and \mathbb{P}_b is bit error rate, which is generally defined by following equation [57]:

$$\mathbb{P}_b(\gamma) = \alpha_M Q\left(\sqrt{\beta_M \gamma}\right), \quad (5.12)$$

where γ indicates Signal to Noise Ratio (SNR), $Q(\cdot)$ denotes the Gaussian Q -function, and α_M and β_M are determined by the type of approximation and modulation (Table 5.2 gives the specific formulae for various modulation schemes).

Eq. (5.12) shows that the bit error rate is a function of γ . On the receiver side, $\gamma = r_{ss} - N_{floor}$, where r_{ss} is the receiver sensitivity and N_{floor} is the noise floor. During signal propagation, the signal power decreases as distance increases. This phenomenon

Table 5.1: Bit error probabilities for modulations

| Modulation | $P_b(\gamma_b)$ |
|-------------|---|
| BFSK | $P_b = Q(\sqrt{\gamma_b})$ |
| BPSK | $P_b = Q(\sqrt{2\gamma_b})$ |
| QPSK, 4-QAM | $P_b \approx Q(\sqrt{2\gamma_b})$ |
| MPAM | $P_b \approx \frac{2(M-1)}{M} Q(\sqrt{\frac{6\gamma_b \log_2 M}{M^2-1}})$ |
| MPSK | $P_b \approx \frac{2}{M \log_2 M} Q(\sqrt{2\gamma_b \log_2 M} \sin(\frac{\pi}{M}))$ |

is statistically modeled using the path loss model $P_L(d)$ defined in Sec. 3.2.2. For the transmission power P_{tx} , the condition $r_{ss} \geq P_{tx} - P_L(d)$ must be guaranteed at the receiver. Thus, r_{ss} can be approximated as $P_{tx} - P_L(d)$. Let $\overline{P_L(d)}$ denote the average path loss in a cluster, i.e., $r_{ss} = P_{tx} - \overline{P_L(d)}$ and $\bar{\gamma} = \theta - \overline{P_L(d)}$, where $\theta = P_{tx} - N_{floor}$. Then, the average PRR , \overline{PRR} , can be derived by substituting $\bar{\gamma}$ for γ for Eq. (5.12) as given below:

$$\overline{PRR}(d) = \left(1 - \alpha_M Q\left(\sqrt{\beta_M (\theta - \overline{P_L(d)})}\right) \right)^{8F}. \quad (5.13)$$

Since a CH is assumed to provide reliable communication using higher transmission power or enhanced low-power long-distance RF module (such as low-power Bluetooth), \overline{PRR} should be optimized for intra-cluster. Within a cluster, CMs can be in one of two possible states: ideal-state and isolated-state. In the ideal state, at least one neighbor node is located within the transmission range of a CM. In contrast, in the isolated-state, there are no relay nodes located within the transmission range of a CM, and thus it has to directly communicate with the CH. The communication reliability of CMs that are in the ideal-state can be guaranteed because the relay nodes are located within their transmission range. On the other hand, CMs that are in the isolated-state will incur many packet retransmissions. Therefore, \overline{PRR} must be derived after obtaining the probabilities

that a node will stay in either the ideal-state or the isolated-state.

In the Poisson 2-D model, the Cumulative Distribution Function (CDF) that the distance of a neighbor node d is smaller than r_{min} is $F(d \leq r_{min}) = 1 - e^{-\pi\lambda r_{min}^2}$. Based on this, the probability that a node remains in the isolated-state can be derived as $1 - F(d \leq r_{min}) = e^{-\pi\lambda r_{min}^2}$, and thus, the probability that a node is in the ideal-state is $1 - e^{-\pi\lambda r_{min}^2}$. For an isolated node, it has to directly communicate with the CH over distance $E[l]$ defined in Eq. (5.5). Based on these results and Eq. (5.13), the average PRR in a cluster is obtained as follow:

$$\begin{aligned} \overline{PRR}(p) &= F(d \leq r_{min}) + (1 - F(d \leq r_{min}))PRR_{isolated} \\ &= \left(1 - e^{-\pi\lambda r_{min}^2}\right) + \\ &\quad e^{-\pi\lambda r_{min}^2} \left(1 - \alpha_M Q \left(\sqrt{\beta_M \left(\theta - P_L \left(\sqrt{\frac{A}{4Np}} \right) \right)} \right) \right)^{8F}, \end{aligned} \quad (5.14)$$

where $PRR_{isolated}$ denotes PRR of the isolated node.

Eq. (5.14) shows that if the modulation scheme as well as $Q(\cdot)$ are known, the average PRR can be optimized in a cluster by determining the appropriate cluster ratio p .

5.2.3 Joint Optimization

The aforementioned analysis shows that an appropriate p potentially improves not only ITC but also \overline{PRR} . However, the results obtained from Theorem 5.2.1 and Eq. (5.14) are independently derived. Therefore, this subsection presents a joint optimization method that optimizes both ITC and \overline{PRR} simultaneously.

Without loss of generality, let $\alpha_M = 1$ and $\beta_M = 1$ (which is valid when the nodes use the FSK modulation scheme, and the specific formula is given in Table 5.2) to compare the impact of p on ITC and \overline{PRR} . This yields the following bit error rate:

$$\mathbb{P}_b(\gamma) = Q(\sqrt{\gamma}) = \frac{1}{2}e^{-\frac{B_n\gamma}{2\eta}}, \quad (5.15)$$

where B_n and η denote the noise bandwidth and transmission rate, respectively. Substituting Eq. (5.15) into Eq. (5.14) results in the following equation for average PRR :

$$\overline{PRR}(p) = \left(1 - e^{-\pi\lambda r_{min}^2}\right) + \left(1 - \frac{1}{2}e^{-\frac{B_n}{2\eta}\left(\theta' - 10k \log_{10} \sqrt{\frac{A}{4Np}}\right)}\right)^{8F}, \quad (5.16)$$

where $\theta' = \theta - 20 \log_{10}(\frac{4\pi}{\omega})$ and ω denotes the wave length.

Fig. 5.1 shows the impact of p and node density on ITC and \overline{PRR} for the $m2s$ (Fig. 5.1(a)) and $m2m$ (Fig. 5.1(b)) cases. As mentioned in Sec. 5.2.1, ITC for the $m2s$ case is not a strictly convex function. This property can be observed from Fig. 5.1(a), where the normalized ITC converges as p increases for the $m2s$ case. Based on this property, the lower bound of the joint optimization solution p^* can be obtained for the $m2s$ case³ with the jointly restricted condition, which is the minimum required communications reliability $PRR_{req} = 98\%$. Using the Lagrangian function, the problem can be converted into a dual problem which is

$$L(p, \mu) = E[ITC_{m2s}(p)] - \mu(\overline{PRR}(p) - 0.98). \quad (5.17)$$

By solving Eq. (5.17), the joint optimization value for p^* that optimizes ITC and guarantees PRR_{req} for various node densities is 0.2, and it can be observed by the analytical results in Fig. 5.1(a).

However, in the $m2m$ case, it is difficult to determine the joint optimization solution p^* with a restricted bound of PRR_{req} to simultaneously optimize ITC and \overline{PRR} . The reason is that the optimized p^* maximizes \overline{PRR} in a cluster by decreasing its area and the distance between CMs and CH. At the same time, the optimized p^* causes the network to be divided into more clusters and thus increases the transmission overhead.

For the $m2m$ case, a low \overline{PRR} will result in excessive packet retransmissions within a cluster. The retransmission count can be derived as $\sum_{i=0}^{j-1} E[H_{tot}(p)] \times (1 - \overline{PRR}(p))^i$,

³In order to distinguish the joint optimization from the normal optimization, notation p^* is used to denote the result of the joint optimization.

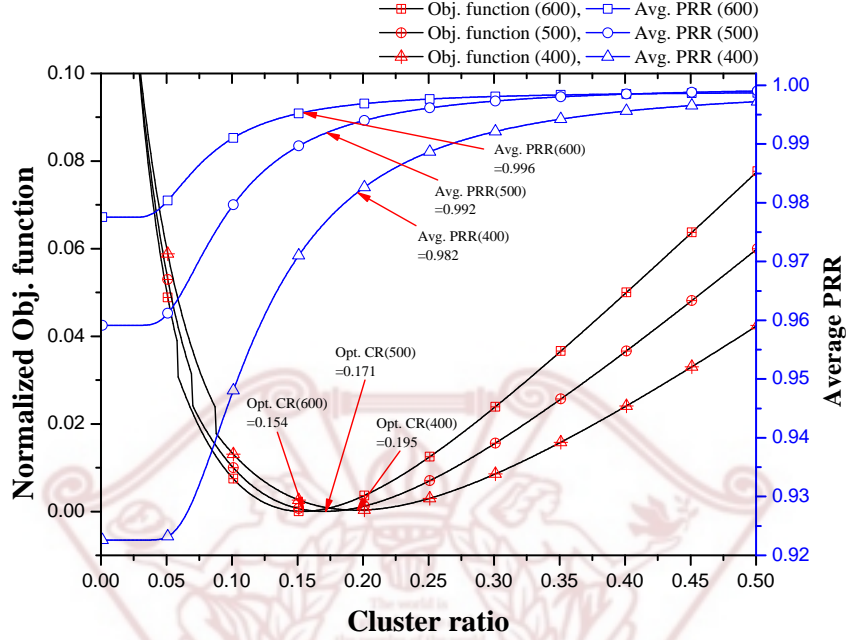


Figure 5.2: Results of joint optimization

where $E[H_{tot}(p)]$ is given by Eq. (5.6), $\overline{PRR}(p)$ is given by Eq. (5.16), and $j = 4$ which indicates the maximum allowable number of retransmissions. On the other hand, the total number of transmissions is the sum of ITC and the number retransmissions. Therefore, the problem of independently optimizing ITC and retransmission count is converted into a problem of minimizing the total transmission count. This is formulated by the following joint optimization function p^* :

$$p^* = \arg \min_{p \in (0,1)} \left(\sum_{i=0}^{j-1} E[H_{tot}(p)] \times (1 - \overline{PRR}(p))^i + E[H_{tot}(p)] \right). \quad (5.18)$$

The objective function in Eq. (5.18) consists of the sum of ITC and retransmission count for the intra-cluster transmission (the first term) and ITC for the inter-cluster transmission (the second term), where the argument p is in the interval $(0, 1)$. Therefore, p^* is obtained that simultaneously minimizes the network transmission hop-count and

maximizes \overline{PRR} with constant time $O(1)$. Fig. 5.2 shows the results of Eq. (5.18), which indicate that the optimal p^* values are 0.195, 0.171, and 0.154 for node densities of 400, 500, and 600, respectively, and the derived p^* can guarantee 98% communication reliability.

5.3 Performance Evaluation

This section compares the performance of the proposed method for determining optimal p^* values against the methods presented in [16, 45] and [46]. The simulated area is $200 \times 200 m^2$ with the sink node located at the center, and the number of randomly deployed nodes are 400, 500, and 600. CHs are also randomly selected based on the given cluster ratio p . Each node selects the closest CH and performs either multi-hop or direct transmission depending on the communication distance. Moreover, each sensor node generates 50-byte packets at a transmission rate of 50 kbps. The network occupies 915 MHz frequency band[26], and transmission power is set to 0 dBm and -25 dBm for intra-cluster and inter-cluster transmission, respectively [58, 59, 60]. The simulator for the performance evaluation is implemented in C.

Table 5.2: Data comparison: Number of nodes deployed is 400

| i -th hop | Simulation results | | | | Approximation results | | | | Difference | | | |
|----------------|--------------------|------|------|------|-----------------------|------|------|------|------------|-------|-------|-------|
| | 0.08 | 0.12 | 0.16 | 0.2 | 0.08 | 0.12 | 0.16 | 0.2 | 0.08 | 0.12 | 0.16 | 0.2 |
| 1 | 2.31 | 2.18 | 1.97 | 1.8 | 2.54 | 2.29 | 2.07 | 1.86 | -0.23 | -0.11 | -0.10 | -0.06 |
| 2 | 3.41 | 2.93 | 2.25 | 1.83 | 4.65 | 3.35 | 2.43 | 1.78 | -1.24 | -0.42 | -0.18 | 0.05 |
| 3 | 2.55 | 1.29 | 0.71 | 0.4 | 2.87 | 1.32 | 0.62 | 0.3 | -0.33 | -0.03 | 0.09 | 0.1 |
| 4 | 1.04 | 0.34 | 0.12 | 0.06 | 0.91 | 0.21 | 0.05 | 0.01 | 0.13 | 0.13 | 0.07 | 0.04 |
| 5 | 0.34 | 0.08 | 0.02 | 0.01 | 0.16 | 0.01 | 0 | 0 | 0.18 | 0.07 | 0.02 | 0.01 |
| 6 | 0.11 | 0.02 | 0.01 | 0 | 0.02 | 0 | 0 | 0 | 0.09 | 0.02 | 0.01 | 0 |

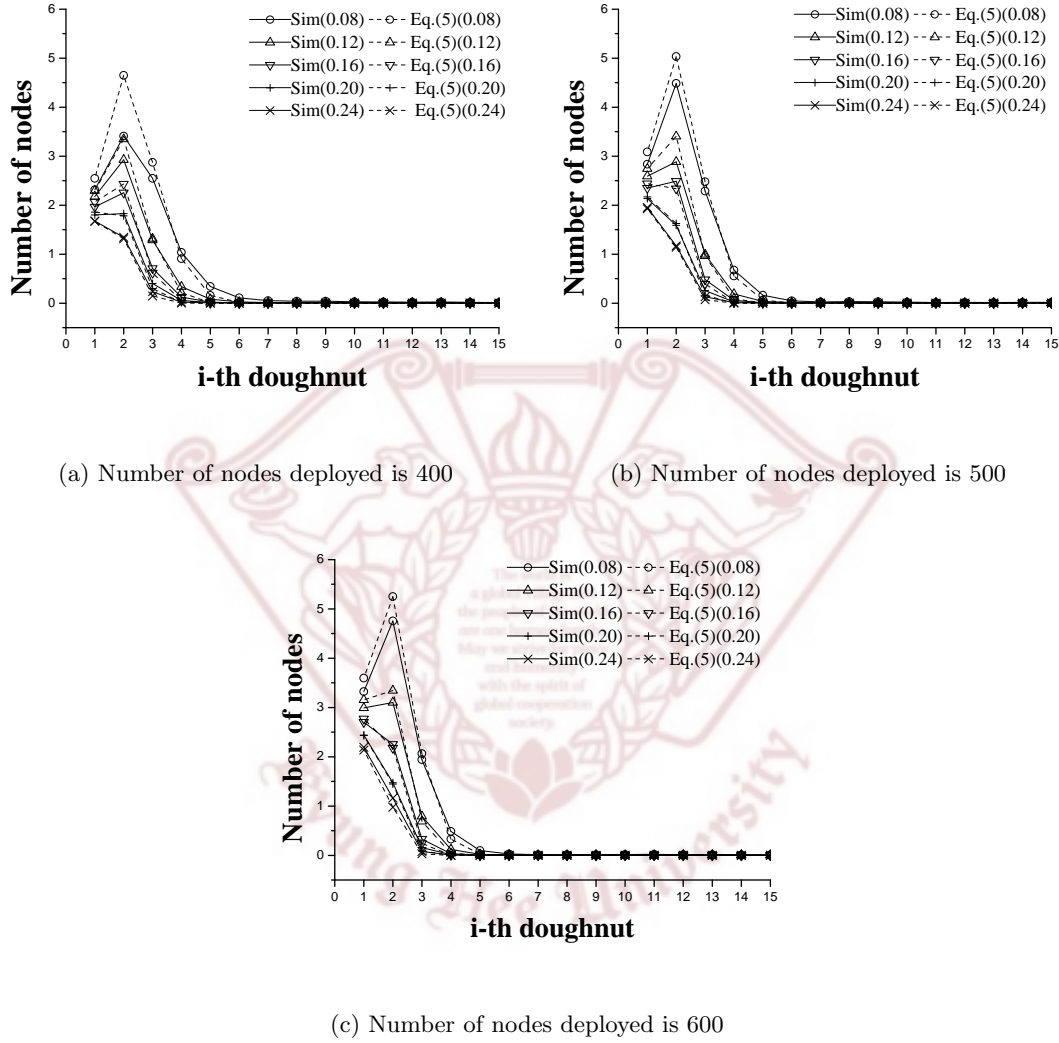


Figure 5.3: Comparison of simulation and approximation results ($r_{min}=10$ m and $p = \{0.08, 0.12, 0.16, 0.2, 0.24\}$)

5.3.1 Validation of the Approximation Efficiency

This subsection validates the approximation efficiency of Eq. (5.2) using simulation. Fig. 5.3 shows the average number of nodes in i -th doughnut, where solid lines denote the

Table 5.3: Data comparison: Number of nodes deployed is 500

| i -th hop | Simulation results | | | | Approximation results | | | | Difference | | | |
|----------------|--------------------|------|------|------|-----------------------|------|------|------|------------|-------|-------|-------|
| | 0.08 | 0.12 | 0.16 | 0.2 | 0.08 | 0.12 | 0.16 | 0.2 | 0.08 | 0.12 | 0.16 | 0.2 |
| 1 | 2.83 | 2.59 | 2.35 | 2.14 | 3.09 | 2.74 | 2.44 | 2.17 | -0.25 | -0.15 | -0.09 | -0.03 |
| 2 | 4.49 | 2.89 | 2.49 | 1.59 | 5.04 | 3.41 | 2.34 | 1.63 | -0.55 | -0.52 | 0.15 | -0.04 |
| 3 | 2.29 | 0.99 | 0.48 | 0.26 | 2.48 | 0.97 | 0.39 | 0.16 | -0.19 | 0.03 | 0.09 | 0.09 |
| 4 | 0.68 | 0.19 | 0.06 | 0.03 | 0.55 | 0.09 | 0.02 | 0 | 0.12 | 0.09 | 0.04 | 0.02 |
| 5 | 0.16 | 0.04 | 0.01 | 0.01 | 0.06 | 0 | 0 | 0 | 0.10 | 0.03 | 0.01 | 0.01 |
| 6 | 0.05 | 0.01 | 0.00 | 0.00 | 0.00 | 0 | 0 | 0 | 0.04 | 0.01 | 0 | 0 |

Table 5.4: Data comparison: Number of nodes deployed is 600

| i -th hop | Simulation results | | | | Approximation results | | | | Difference | | | |
|----------------|--------------------|------|------|------|-----------------------|------|------|------|------------|-------|-------|------|
| | 0.08 | 0.12 | 0.16 | 0.2 | 0.08 | 0.12 | 0.16 | 0.2 | 0.08 | 0.12 | 0.16 | 0.2 |
| 1 | 3.32 | 2.99 | 2.70 | 2.44 | 3.60 | 3.15 | 2.77 | 2.43 | -0.27 | -0.16 | -0.07 | 0.01 |
| 2 | 4.76 | 3.1 | 2.25 | 1.48 | 5.25 | 3.35 | 2.18 | 1.45 | -0.49 | -0.24 | 0.07 | 0.03 |
| 3 | 1.94 | 0.79 | 0.33 | 0.16 | 2.07 | 0.69 | 0.24 | 0.09 | -0.12 | 0.1 | 0.09 | 0.07 |
| 4 | 0.48 | 0.12 | 0.03 | 0.01 | 0.33 | 0.04 | 0.01 | 0 | 0.16 | 0.08 | 0.03 | 0.01 |
| 5 | 0.1 | 0.02 | 0.01 | 0 | 0.02 | 0 | 0 | 0 | 0.07 | 0.02 | 0.01 | 0 |
| 6 | 0.03 | 0.01 | 0.01 | 0 | 0 | 0 | 0 | 0 | 0.03 | 0.01 | 0.01 | 0 |

simulation results (which are averages of 200 runs) and dash lines denote the calculated results of Eq. (5.2). Eq. (5.2) takes the i -th hop as well as the density of cluster head and cluster members, which is based on p , as input parameters and calculates the results for different values of p , i.e., 0.08, 0.12, 0.16, 0.2, and 0.24.

The following two observations can be made from Fig. 5.3. The first is the impact of node density on the approximation efficiency. Our results show that the approximation

accuracy increases as node density increases. The second is that the approximation error can be ignored if p is sufficiently large. For example, although the node density is low in Fig. 5.3(a), the approximation results are close to the simulation results (specific differences between simulation and approximation results are listed in Tables 5.2, 5.3 and 5.4.) when $p > 0.08$, and the proposed optimization point, p^* , is greater than 0.08 as presented in Sec. 5.2.3 (i.e., $p^* = 0.2$ in the $m2s$ case and $p^* = \{0.195, 0.171, 0.154\}$ in the $m2m$ case). Therefore, the approximation suffers from only few interference errors.

In addition to the data analyses in large-scale applications, dispersion degrees of the approximation results in relatively smaller area are shown in Table 5.5 (CR is set to 0.2). Root Mean Square Error (RMSE) is selected as the performance metric, and the number of nodes, N , deployed in the networks is determined based on the lower bound of the deployed node density which should be efficient to guarantee that there are no isolate sensor nodes in the networks. Through comparing RMSE values in Table 5.5, we can observe that the approximation results are approached to the simulation results with the area, A , is increased. More details can be observed by utilizing the parameter 4σ which denotes an error bound. For the random errors, 4σ is useful for evaluating the dispersion degree of the approximation results because the results includes in the interval $x - 4\sigma < \hat{x} < x + 4\sigma$ with probability 0.9999 (where x and \hat{x} indicate the real value and measured value, respectively). Data in 4σ row shows that the approximation result is nearly dispersed in the interval $[-1, +1]$ in $10^2 m^2$ and $50^2 m^2$ area. For the relatively larger area, i.e., $100^2 m^2$ and $200^2 m^2$, there are more random events which are counting the number of nodes in the donuts are occurred and randomness can be easily found. Therefore, the approximation suffers from only few interference errors, and the error bound is close to or lower than 0.2. Consequentially, the dispersively of the approximation is acceptable with small error bound in the large area which is equal or greater than $100^2 m^2$.

Table 5.5: RMSE for different environments

| Environment | RMSE (σ) | 4σ |
|---|-------------------|-----------|
| $10 \times 10 \text{ m}^2$ (A), 20 (N) | 0.281 | 1.123 |
| $10 \times 10 \text{ m}^2$ (A), 30 (N) | 0.222 | 0.889 |
| $50 \times 50 \text{ m}^2$ (A), 50 (N) | 0.218 | 0.871 |
| $50 \times 50 \text{ m}^2$ (A), 100 (N) | 0.182 | 0.727 |
| $100 \times 100 \text{ m}^2$ (A), 200 (N) | 0.051 | 0.206 |
| $100 \times 100 \text{ m}^2$ (A), 400 (N) | 0.043 | 0.173 |
| $200 \times 200 \text{ m}^2$ (A), 600 (N) | 0.025 | 0.1 |

5.3.2 Performance of the Proposed Joint Optimization

This subsection compares the performance of the optimized p based on the ITC function in Eq. (5.9) and the proposed joint optimization function in Eq. (5.18). Based on Eqs. (5.9) and (5.18), the optimal p and p^* for the three node densities are $\{0.183, 0.165, 0.15\}$ and $\{0.195, 0.171, 0.154\}$, respectively. In order to provide a fair performance comparison, the data generation in the simulation is set so that each node in the network sequentially generates one packet and sends it to the sink node.

Fig. 5.4 compares the ITC values obtained from the proposed joint optimization scheme and optimizing only the ITC function for various node densities. The numbers on histograms are used to indicate the optimal p which are obtained by the analytic models. These results show that the optimal p^* obtained using the joint optimization scheme can reduce ITC by 2.18%, 1.68%, and 1.14% compare to p obtained from only optimizing the ITC function. Fig. 5.5 shows that the communication reliability is also enhanced by the joint optimization. The reason for this is that the proposed method simultaneously optimizes the network ITC and PRR , and thus, higher PRR is guaranteed and

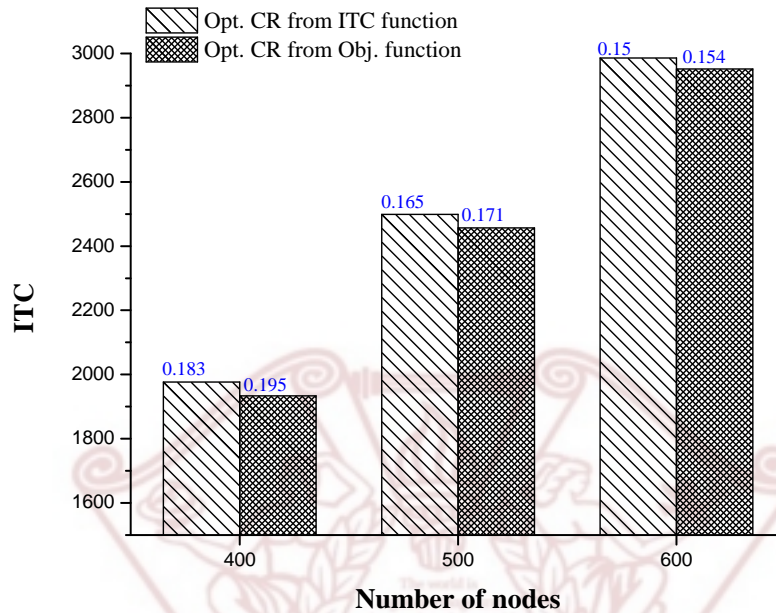


Figure 5.4: Comparison of the network ITC for different node densities

the number of retransmissions is effectively reduced resulting in lower ITC . Therefore, these results verify that the proposed joint optimization leads to a more energy efficient network.

5.3.3 Comparison with Existing Analytic Models

This subsection compares the proposed joint optimization with the existing analytical models by Kumar *et al.* [16, 45] and Bandyopadhyay *et al.* [46]. According to their results, the optimal p values are $\{0.06, 0.054, 0.049\}$ [16, 45], and $\{0.101, 0.093, 0.087\}$ [46] for the three node densities.

Fig. 5.6 shows the network ITC results for different optimum p and p^* values and node densities. The figure shows that the cluster ratio optimization techniques proposed in [16, 45] and [46] do not minimize the network ITC . The reason is that the analytic

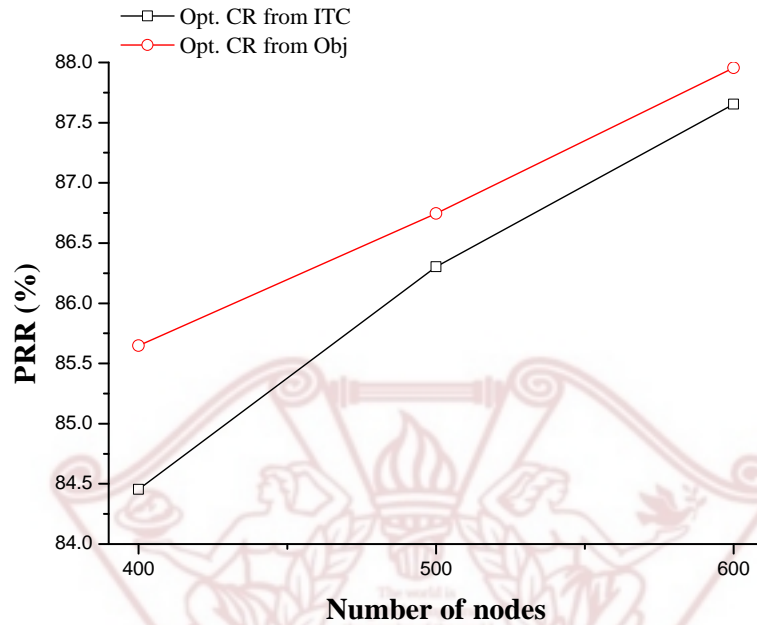
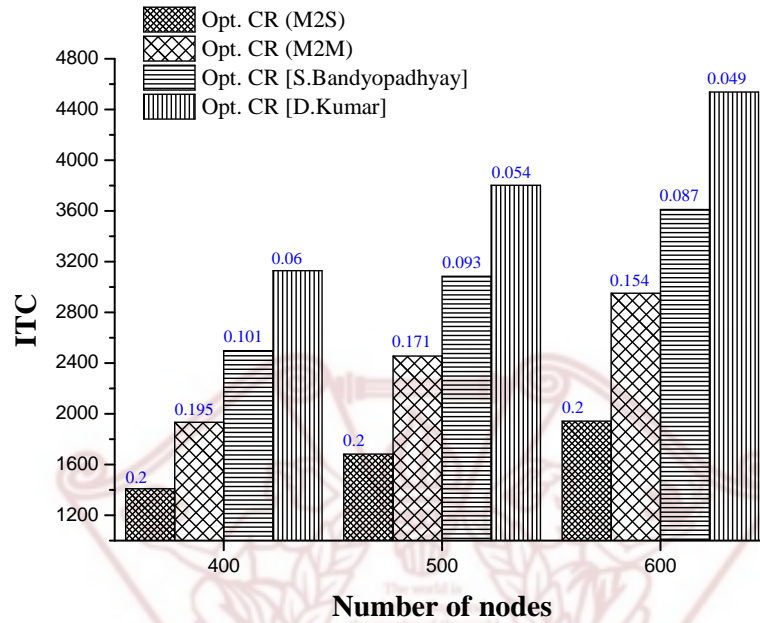


Figure 5.5: Comparison of the average PRR for different node densities

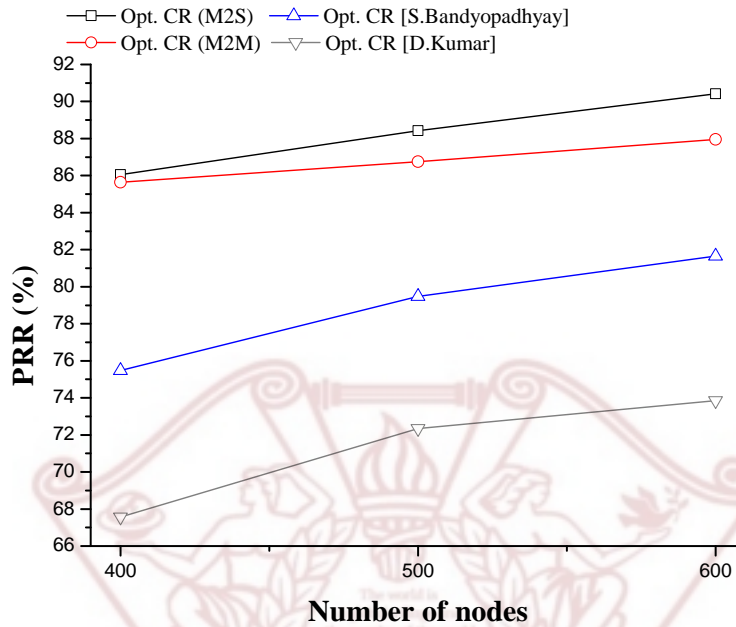
model in [16, 45] is an extension of LEACH for multi-hop communications, which does not take into account the important factors in energy efficiency, which are ITC and PRR . The optimization technique proposed by Bandyopadhyay *et al.* [46] shows better performance than the one provided in [16, 45], and this is because their analysis is performed with minimizing the network ITC in mind. However, there is a performance gap between the optimal p^* provided by the proposed joint optimization scheme and the one by Bandyopadhyay *et al.* This gap is caused by their estimation errors, and is also related to the fact that they do not take communication reliability into consideration.

Fig. 5.7 shows the average PRR for the three node densities. This figure shows that the existing optimization techniques result in low average PRR , and this will cause a lot of packet retransmissions and extra energy dissipation. With an improper choice of p , the average PRR will be low as shown in the mathematical analysis results in Fig. 5.1, and

Figure 5.6: Network *ITC*

it becomes worse as the hop-count increases. As shown in Fig. 5.7, the average *PRR* can be improved by increasing the node density. The reason is that if nodes are more densely deployed, the probability of maintaining good communication links increases. However, simply increasing node density is not feasible in most applications. Therefore, properly setting the p value is a more efficient way to improve the network *PRR* and enhance network energy efficiency.

These simulation results also show that the performance improvement in *m2s* is higher than *m2m*. This is because low-power, long-distance RF module is assumed in *m2s*; therefore, the connection between CHs and the sink node is ideal, and thus *ITC* is equal to the number of CHs, which is lower than for multi-hop communications.

Figure 5.7: Average PRR

5.3.4 Network Life Time

This subsection studies the impact of various cluster ratio optimization techniques on the network energy efficiency. In order to evaluate energy consumption, simulation is performed for 100 iterations, and in each iteration, each sensor node sends 1000 packets to the sink node. In this thesis, the network life time is defined as the time until the FND (First Node “Dead”) [13]. The initialized energy is set to 10 J, and the abstract time is represented by a more specific metric, which is the number of packets received at the sink node before FND.

Fig. 5.8 shows that the proposed joint optimization technique significantly reduces the energy consumption of sensor nodes, which clearly indicates the benefits of optimizing both ITC and PRR .

Fig. 5.9 shows that proposed analytical model outperforms existing schemes in terms

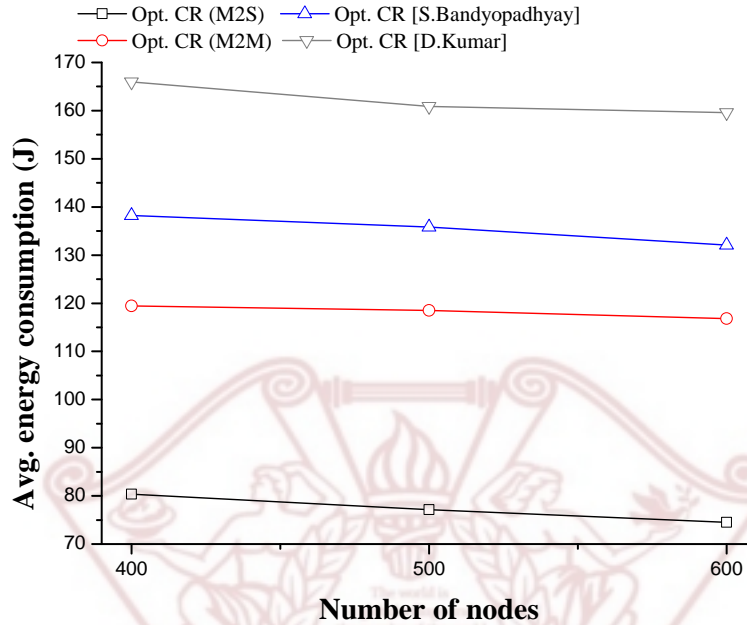


Figure 5.8: Average energy consumption

of network lifetime. By setting optimal p^* , the number of received packets is approximately 14% ~ 39% higher than the methods in [16, 45] and [46] for the *m2m* case. The results for the *m2s* case is significantly better than the existing methods (by at least 72%) because data from each sensor node is aggregate at a CH and then transmitted directly to the sink node.

Our study shows that the proposed joint optimization technique significantly improves the network energy efficiency in term of *ITC* and *PRR*, and increases the network life-time. Another notable result is that energy efficiency of the *m2s* case is better than the *m2m* case. This is because even though more energy is consumed during long distance transmissions, the benefits of lower *ITC* and higher average *PRR* lead to longer network life time than the *m2m* case.

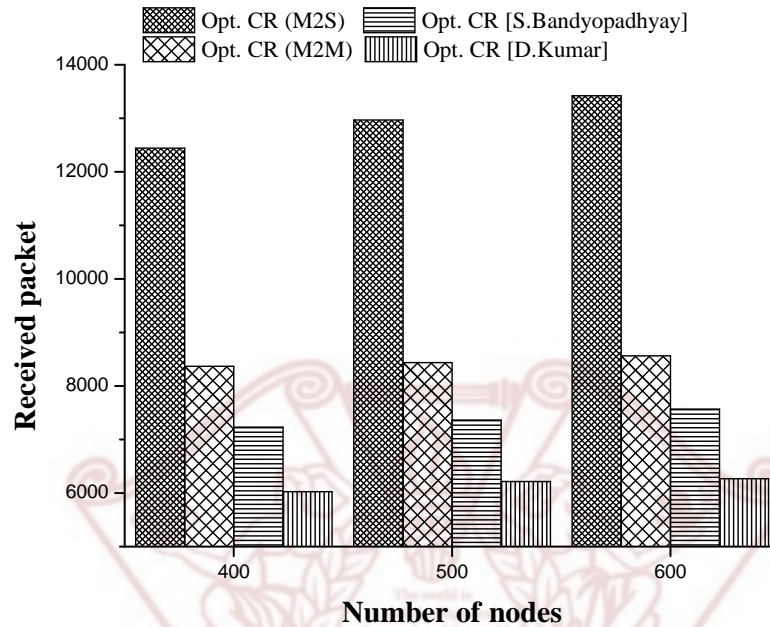


Figure 5.9: Received packet before FND

5.4 Summary

This chapter presented a novel analytic model to analyze the optimal CR for cluster-based WSNs to enhance the network energy efficiency. The derived optimal CR can be applied in the applications of WSN in large scale area such as environmental monitoring, battle field and border surveillance for optimizing the network energy efficiency. The applications area and node density are utilized as input variable for the analytic model, and after performing the optimization, the network structure can be carefully planned to achieve the optimal network life time before deploying the network to a target area.

The specific methodology for developing the analytic model is that the impact of CR on the network performance was analyzed without any specific assumptions about energy models and network environment. Furthermore, the analysis considers various data propagation models. Therefore, the analysis is applicable to generic cluster-based WSNs.

Based on the analytic model, a joint optimization scheme was proposed to improve the network energy efficiency by simultaneously optimizing *ITC* and *PRR*. The performance of the optimal *CR* derived using the proposed joint optimization scheme was validated through simulations. Our simulation results clearly showed the benefits of the optimal *CR* over existing optimization methods in terms of *PRR* and energy efficiency.



Chapter 6

Conclusions and Future Work

In this chapter, we conclude the research results presented in this thesis and suggest few directions for future work.

6.1 Conclusions

In this thesis, analytic models were developed based on mathematically analyzing the stochastic properties of the three-level hierarchy wireless networks. Specifically, the developed analytic models are efficient to optimize transmission efficiency of the three-level hierarchy networks in terms of the networks' costs and energy efficiency. The analytic models also address the design of public network infrastructure, and incorporate more generalized constraints to allow the network planner a higher degree of freedom in planning the network deployment and structure on local requirements. In order to guarantee the analytic models' applicability, the hypothesis parameters were limited through mathematically modeling the networks. Furthermore, the common characteristic of spatial structure of the three-level hierarchy networks was taken into account in the analytic models to normalize the analyses.

Besides the above mentioned common contributions of this thesis the specific achievement are summarized in two parts.

First, this thesis analyzed the impact of the number of RSs on the average link length between user and RS, and then derived an analytic model to determine the lower bound on

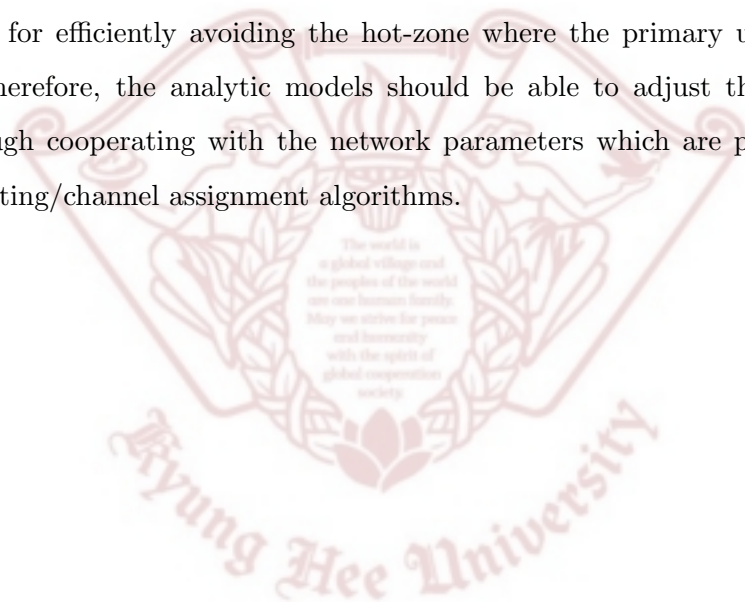
the number of distributed RSs and the optimal number of RSs for various levels of MCS. The proposed scheme was validated through a set of simulations. When we consider both cost-effectiveness and users' QoS requirement at the same time, our scheme can provide an effective solution on the optimal number of RSs.

Second, this thesis presented a novel analytic model to analyze the optimal CR for cluster-based WSNs to enhance the network energy efficiency. The impact of CR on the network performance was analyzed without any specific assumptions about energy models and network environment. Furthermore, the analysis considers various data propagation models. Therefore, the analysis is applicable to generic cluster-based WSNs. Based on the analytic model, a joint optimization scheme was proposed to improve the network energy efficiency by simultaneously optimizing ITC and PRR . The performance of the optimal CR derived using the proposed joint optimization scheme was validated through simulations. Our simulation results clearly showed the benefits of the optimal CR over existing optimization methods in terms of PRR and energy efficiency.

6.2 Future Work

In the foreseeable future, tens of billions of electronic devices will be expected to communicate with each other and require a huge amount of radio resources. However, the current radio resources is lack of due to inflexible spectrum sharing rules, and the existing wireless networks, such as WLANs, mesh networks, wireless body area networks, and WSNs, which operate in unlicensed band will suffer from serious spectrum overcrowding problem. The cognitive radio technology that exploits dynamic spectrum access scheme is a promising solution to solving this problem. Currently, There are many excellent research focused on designing efficient communication protocols for the cognitive radio based distributed networks, i.e., cognitive radio ad-hoc networks and Cognitive Radio Sensor Networks (CRSNs) [61, 62, 63].

Our future plan is to extend the proposed analytic models to involve the feature of dynamic spectrum access in the cognitive radio based distributed wireless networks. Due to the available channels in a local area are significantly affected by the behavior of primary users, the network topology is no more stable, and thus it makes the proposed mathematical analysis infeasible. For solving this challenge, the analytic model should take influence of the primary user into account. Furthermore, data propagation models will be more complicated because more intelligent routing algorithms are required in network layer for efficiently avoiding the hot-zone where the primary users frequently appeared. Therefore, the analytic models should be able to adjust the optimization solution through cooperating with the network parameters which are provided by the intelligent routing/channel assignment algorithms.



Bibliography

- [1] K. Park, K. Lee, S. Park, and H. Lee, "Telecommunication node clustering with node compatibility and network survivability requirements," *Management Science, INFORMS*, vol. 46, no. 3, pp. 363–374, 2000.
- [2] X. Wu, B. M. Jee, and D. Ghosal, "Hierarchical architectures in the third-generation cellular network," *Wireless Communications, IEEE*, vol. 11, no. 3, pp. 62–71, 2004.
- [3] K. Lu, Y. Qian, and H. Chen, "Wireless broadband access: Wimax and beyond-a secure and service-oriented network control framework for wimax networks," *Communications Magazine, IEEE*, vol. 45, no. 5, pp. 124–130, 2007.
- [4] A. K. Sadek, Z. Han, and K. Liu, "Distributed relay-assignment protocols for coverage expansion in cooperative wireless networks," *Mobile Computing, IEEE Transactions on*, vol. 9, no. 4, pp. 505–515, 2010.
- [5] D. Soldani and S. Dixit, "Wireless relays for broadband access," *Communications Magazine, IEEE*, vol. 46, no. 3, pp. 58–66, 2008.
- [6] Z. Jin, W. Su, J. Cho, and E.-K. Hong, "An analytic model for the optimal number of relay stations in two-hop relay networks," *Communications Letters, IEEE*, vol. 17, no. 2, pp. 285–288, 2013.
- [7] I. F. Akyildiz, W. Su, Y. Sankarasubramaniam, and E. Cayirci, "A survey on sensor networks," *Communications magazine, IEEE*, vol. 40, no. 8, pp. 102–114, 2002.

- [8] A. A. Abbasi and M. Younis, "A survey on clustering algorithms for wireless sensor networks," *Computer communications*, vol. 30, no. 14, pp. 2826–2841, 2007.
- [9] Y.-K. Huang, A.-C. Pang, P.-C. Hsiu, W. Zhuang, and P. Liu, "Distributed throughput optimization for zigbee cluster-tree networks," *Parallel and Distributed Systems, IEEE Transactions on*, vol. 23, no. 3, pp. 513–520, 2012.
- [10] H. Lu, J. Li, and M. Guizani, "Secure and efficient data transmission for cluster-based wireless sensor networks," *Parallel and Distributed Systems, IEEE Transactions on*, vol. 25, no. 3, pp. 750–761, 2014.
- [11] M. Noori and M. Ardakani, "Lifetime analysis of random event-driven clustered wireless sensor networks," *Mobile Computing, IEEE Transactions on*, vol. 10, no. 10, pp. 1448–1458, 2011.
- [12] H. Shen, Z. Li, L. Yu, and C. Qiu, "Efficient data collection for large-scale mobile monitoring applications," *Parallel and Distributed Systems, IEEE Transactions on*, vol. 25, no. 6, pp. 1424–1436, 2014.
- [13] W. B. Heinzelman, A. P. Chandrakasan, and H. Balakrishnan, "An application-specific protocol architecture for wireless microsensor networks," *Wireless Communications, IEEE Transactions on*, vol. 1, no. 4, pp. 660–670, 2002.
- [14] H. Yang and B. Sikdar, "Optimal cluster head selection in the leach architecture," in *Performance, Computing, and Communications Conference, 2007. IPCCC 2007. IEEE International*. IEEE, 2007, pp. 93–100.
- [15] B. Chen, Y. Zhang, Y. Li, X. Hao, and Y. Fang, "A clustering algorithm of cluster-head optimization for wireless sensor networks based on energy," *Journal of Information & Computational Science*, vol. 8, no. 11, pp. 2129–2136, 2011.

- [16] D. Kumar, T. C. Aseri, and R. Patel, "EEHC: Energy efficient heterogeneous clustered scheme for wireless sensor networks," *Computer Communications*, vol. 32, no. 4, pp. 662–667, 2009.
- [17] R. Xie and X. Jia, "Transmission-efficient clustering method for wireless sensor networks using compressive sensing," *Parallel and Distributed Systems, IEEE Transactions on*, vol. 25, no. 3, pp. 806–815, 2014.
- [18] Y. P. Chen, A. L. Liestman, and J. Liu, "Energy-efficient data aggregation hierarchy for wireless sensor networks," in *Quality of Service in Heterogeneous Wired/Wireless Networks, 2005. Second International Conference on*. IEEE, 2005, pp. 7–7.
- [19] Z. Jin, D.-Y. Kim, J. Cho, and B. Lee, "An analysis on optimal cluster ratio in cluster-based wireless sensor networks," *Sensors Journal, IEEE*, vol. 15, no. 11, pp. 6413–6423, 2015.
- [20] K. R. Liu, *Cooperative communications and networking, Ch.4*. Cambridge university press, 2009.
- [21] E. M. Belding-Royer, "Hierarchical routing in ad hoc mobile networks," *Wireless Communications and Mobile Computing*, vol. 2, no. 5, pp. 515–532, 2002.
- [22] Z. H. Khan, D. G. Catalot, and J. M. Thiriet, "Hierarchical wireless network architecture for distributed applications," in *Wireless and Mobile Communications, 2009. ICWMC'09. Fifth International Conference on*. IEEE, 2009, pp. 70–75.
- [23] J. Zheng and A. Jamalipour, *Wireless sensor networks: a networking perspective, Ch.6*. John Wiley & Sons, 2009.
- [24] G. J. Pottie and W. J. Kaiser, "Wireless integrated network sensors," *Communications of the ACM*, vol. 43, no. 5, pp. 51–58, 2000.

- [25] L. Meng, H. Zhang, and Y. Zou, "A data aggregation transfer protocol based on clustering and data prediction in wireless sensor networks," in *Wireless Communications, Networking and Mobile Computing (WiCOM), 2011 7th International Conference on*. IEEE, 2011, pp. 1–5.
- [26] V. Genc, S. Murphy, Y. Yu, and J. Murphy, "IEEE 802.16J relay-based wireless access networks: an overview," *Wireless Communications, IEEE*, vol. 15, no. 5, pp. 56–63, 2008.
- [27] D. Li and H. Jin, "Relay selection in two-hop IEEE 802.16 mobile multi-hop relay networks," in *Education Technology and Computer Science, 2009. ETCS'09. First International Workshop on*, vol. 2. IEEE, 2009, pp. 1007–1011.
- [28] S. Kadloor and R. Adve, "Optimal relay assignment and power allocation in selection based cooperative cellular networks," in *Communications, 2009. ICC'09. IEEE International Conference on*. IEEE, 2009, pp. 1–5.
- [29] Y. Shi, S. Sharma, Y. T. Hou, and S. Kompella, "Optimal relay assignment for cooperative communications," in *Proceedings of the 9th ACM international symposium on Mobile ad hoc networking and computing*. ACM, 2008, pp. 3–12.
- [30] M. Yuanyuan, Z. Sihai, and Z. Wuyang, "Joint channel-topology based opportunistic relay selection strategy," in *Wireless Communications & Signal Processing, 2009. WCSP 2009. International Conference on*. IEEE, 2009, pp. 1–4.
- [31] H. Zhang, W. Wang, D. Liang, and M. Peng, "A cross-layer relay selection algorithm for infrastructure-based two-hop relay networks," in *Communication Software and Networks, 2009. ICCSN'09. International Conference on*. IEEE, 2009, pp. 77–81.
- [32] E. Beres and R. Adve, "Selection cooperation in multi-source cooperative networks," *Wireless Communications, IEEE Transactions on*, vol. 7, no. 1, pp. 118–127, 2008.

- [33] D. S. Michalopoulos and G. K. Karagiannidis, "Performance analysis of single relay selection in rayleigh fading," *Wireless Communications, IEEE Transactions on*, vol. 7, no. 10, pp. 3718–3724, 2008.
- [34] Y. Wei, F. R. Yu, and M. Song, "Distributed optimal relay selection in wireless cooperative networks with finite-state markov channels," *Vehicular Technology, IEEE Transactions on*, vol. 59, no. 5, pp. 2149–2158, 2010.
- [35] Y. Dong, Y. Zhang, M. Song, Y. Teng, and Y. Man, "Optimal relay location in OFDMA based cooperative networks," in *Wireless Communications, Networking and Mobile Computing, 2009. WiCom'09. 5th International Conference on*. IEEE, 2009, pp. 1–4.
- [36] Y. Ge, S. Wen, and Y.-H. Ang, "Analysis of optimal relay selection in IEEE 802.16 multihop relay networks," in *Wireless Communications and Networking Conference, 2009. WCNC 2009. IEEE*. IEEE, 2009, pp. 1–6.
- [37] Y. Yang, X. Wang, and X. Cai, "On the number of relays for orthogonalize-and-forward relaying," in *Wireless Communications and Signal Processing (WCSP), 2011 International Conference on*. IEEE, 2011, pp. 1–5.
- [38] A. So and B. Liang, "Effect of relaying on capacity improvement in wireless local area networks," in *Wireless Communications and Networking Conference, 2005 IEEE*, vol. 3. IEEE, 2005, pp. 1539–1544.
- [39] Y. Wang, G. Feng, and Y. Zhang, "Cost-efficient deployment of relays for lte-advanced cellular networks," in *Communications (ICC), 2011 IEEE International Conference on*. IEEE, 2011, pp. 1–5.
- [40] V. Genc, S. Murphy, and J. Murphy, "An interference-aware analytical model for performance analysis of transparent mode 802.16 j systems," in *GLOBECOM Workshops, 2008 IEEE*. IEEE, 2008, pp. 1–6.

- [41] O. Younis and S. Fahmy, "HEED: a hybrid, energy-efficient, distributed clustering approach for ad hoc sensor networks," *Mobile Computing, IEEE Transactions on*, vol. 3, no. 4, pp. 366–379, 2004.
- [42] D. Wei, Y. Jin, S. Vural, K. Moessner, and R. Tafazolli, "An energy-efficient clustering solution for wireless sensor networks," *Wireless Communications, IEEE Transactions on*, vol. 10, no. 11, pp. 3973–3983, 2011.
- [43] S. Manisekaran and R. Venkatesan, "An adaptive distributed power efficient clustering algorithm for wireless sensor networks," *American Journal of Scientific Research*, no. 10, pp. 50–63, 2010.
- [44] K. T. Kim, H. K. Yoo, B. H. Son, and H. Y. Youn, "An energy efficient clustering scheme for self-organizing distributed wireless sensor networks," in *Computer and Information Technology (CIT), 2010 IEEE 10th International Conference on*. IEEE, 2010, pp. 1468–1473.
- [45] D. Kumar, "Performance analysis of energy efficient clustering protocols for maximising lifetime of wireless sensor networks," *Wireless Sensor Systems, IET*, vol. 4, no. 1, pp. 9–16, 2014.
- [46] S. Bandyopadhyay and E. J. Coyle, "An energy efficient hierarchical clustering algorithm for wireless sensor networks," in *INFOCOM 2003. Twenty-Second Annual Joint Conference of the IEEE Computer and Communications. IEEE Societies*, vol. 3. IEEE, 2003, pp. 1713–1723.
- [47] S. Foss and S. Zuyev, "On a Voronoi aggregative process related to a bivariate poisson process," *Advances in Applied Probability*, pp. 965–981, 1996.
- [48] G. Senarath, W. Tong, P. Zhu, H. Zhang, D. Steer, D. Yu, M. Naden, and D. Kitchenner, "Multi-hop relay system evaluation methodology (channel model and performance metric)," *IEEE C802. 16j-06/013r3*, 2007.

- [49] S. N. Chiu, D. Stoyan, W. S. Kendall, and J. Mecke, *Stochastic geometry and its applications, Ch.4.* John Wiley & Sons, 2013.
- [50] L. S. Committee *et al.*, “IEEE standard for information technology telecommunications and information exchange between systems local and metropolitan area networks specific requirements. part 15.4: wireless Medium Access Control (MAC) and Physical Layer (PHY) specifications for Low-Rate Wireless Personal Area Networks (LR-WPANs),” *IEEE Std*, vol. 802, 2006.
- [51] V. Erceg, L. J. Greenstein, S. Y. Tjandra, S. R. Parkoff, A. Gupta, B. Kulic, A. Julius, R. Bianchi *et al.*, “An empirically based path loss model for wireless channels in suburban environments,” *Selected Areas in Communications, IEEE Journal on*, vol. 17, no. 7, pp. 1205–1211, 1999.
- [52] Y. Kim and H. Liu, “Infrastructure relay transmission with cooperative MIMO,” *Vehicular Technology, IEEE Transactions on*, vol. 57, no. 4, pp. 2180–2188, 2008.
- [53] W. ForumTM, “Mobile WiMAX–Part 1: A technical overview and performance evaluation,” *White Paper, June*, vol. 2, p. 15, 2006.
- [54] T. Ying, Z. Shu-Fang, and W. Ying, “A distributed protocol for ensuring both probabilistic coverage and connectivity of high density wireless sensor networks,” in *Wireless Communications and Networking Conference, 2008. WCNC 2008. IEEE*. IEEE, 2008, pp. 2069–2074.
- [55] M. Khanjary, M. Sabaei, and M. R. Meybodi, “Critical density for coverage and connectivity in two-dimensional aligned-orientation directional sensor networks using continuum percolation,” *Sensors Journal, IEEE*, vol. 14, no. 8, pp. 2856–2863, 2014.
- [56] H. Cai, X. Jia, and M. Sha, “Critical sensor density for partial connectivity in large area wireless sensor networks,” *ACM Transactions on Sensor Networks (TOSN)*, vol. 7, no. 4, p. 35, 2011.

- [57] A. Goldsmith, *Wireless communications, Ch.6*. Cambridge university press, 2005.
- [58] D.-Y. Kim, Z. Jin, J. Choi, B. Lee, and J. Cho, "Transmission power control with the guaranteed communication reliability in wsn," *International Journal of Distributed Sensor Networks*, vol. 2015, 2015.
- [59] Q. Wang, M. Hempstead, and W. Yang, "A realistic power consumption model for wireless sensor network devices," in *Sensor and Ad Hoc Communications and Networks, 2006. SECON'06. 2006 3rd Annual IEEE Communications Society on*, vol. 1. IEEE, 2006, pp. 286–295.
- [60] S. Lin, J. Zhang, G. Zhou, L. Gu, J. A. Stankovic, and T. He, "ATPC: adaptive transmission power control for wireless sensor networks," in *Proceedings of the 4th international conference on Embedded networked sensor systems*. ACM, 2006, pp. 223–236.
- [61] Z. Jin, D. Guan, J. Cho, and B. Lee, "A routing algorithm based on semi-supervised learning for cognitive radio sensor networks." in *SENSORNETS*, 2014, pp. 188–194.
- [62] M. Cesana, F. Cuomo, and E. Ekici, "Routing in cognitive radio networks: Challenges and solutions," *Ad Hoc Networks*, vol. 9, no. 3, pp. 228–248, 2011.
- [63] R. Yu, Y. Zhang, W. Yao, L. Song, and S. Xie, "Spectrum-aware routing for reliable end-to-end communications in cognitive sensor network," in *Global Telecommunications Conference (GLOBECOM 2010), 2010 IEEE*. IEEE, 2010, pp. 1–5.

Appendix A

Proof of Formula (5.2)

In a given cluster, CH_i , the expected number of CMs within radius r' , $E[N_{r'}]$, can be derived as

$$E[N_{r'}] = \int_0^{r'} \lambda_{CM} 2\pi l \mathbf{P}(CM_j \in CH_i) dl, \quad (\text{A.1})$$

where $\mathbf{P}(\cdot)$ denotes a Plam distribution. The sensor nodes are deployed within the network based on a homogeneous Poisson point process, and CM_j belongs to CH_i if and only if a disc with the radius l around CM_i does not contain any other CHs. Therefore, $\mathbf{P}(CM_j \in CH_i) = e^{-\lambda_{CH}\pi l^2}$ and Eq. (A.1) can be rewritten as shown below:

$$\begin{aligned} E[N_{r'}] &= \lambda_{CM} 2\pi \int_0^{r'} l e^{-\lambda_{CH}\pi l^2} dl, \\ &= \frac{\lambda_{CM}}{\lambda_{CH}} (1 - e^{-\lambda_{CH}\pi r'^2}). \end{aligned} \quad (\text{A.2})$$

When $r' \rightarrow \infty$, $e^{-\lambda_{CH}\pi r'^2} = 0$ and thus $E[N_{r'}] = E[N_{tot}] = \frac{\lambda_{CM}}{\lambda_{CH}}$. (A complete proof of Eq. (5.1) (or Eq. (A.2)) is given in [47].)

According to Eq. (A.2), the expected number of CMs within radiuses r_{min} and $2r_{min}$ are $\frac{\lambda_{CM}}{\lambda_{CH}}(1 - e^{-\lambda_{CH}\pi r_{min}^2})$ and $\frac{\lambda_{CM}}{\lambda_{CH}}(1 - e^{-\lambda_{CH}\pi (2r_{min})^2})$, respectively. Suppose the region of the i -th donut is defined as $\pi(ir_{min})^2 - \pi((i-1)r_{min})^2$, then the expected number of CMs in the 2-nd donut ($i = 2$), $E[N_{CM}^2]$, is given as

$$\begin{aligned} E[N_{CM}^2] &= \frac{\lambda_{CM}}{\lambda_{CH}} (1 - e^{-\lambda_{CH}\pi (2r_{min})^2}) - \\ &\quad \frac{\lambda_{CM}}{\lambda_{CH}} (1 - e^{-\lambda_{CH}\pi r_{min}^2}) \\ &= \frac{\lambda_{CM}}{\lambda_{CH}} (e^{-\lambda_{CH}\pi r_{min}^2} - e^{-\lambda_{CH}\pi (2r_{min})^2}). \end{aligned} \quad (\text{A.3})$$

Using the same method that analyzes the expected number for the simple case (where $i = 2$), Eq. (A.3) can be normalized to a general case for a non-negative integer, i .

$$\begin{aligned} E[N_{CM}^i] &= \frac{\lambda_{CM}}{\lambda_{CH}} (1 - e^{-\lambda_{CH}\pi(ir_{min})^2}) - \\ &\quad \frac{\lambda_{CM}}{\lambda_{CH}} (1 - e^{-\lambda_{CH}\pi((i-1)r_{min})^2}) \\ &= \frac{\lambda_{CM}}{\lambda_{CH}} (e^{-\lambda_{CH}\pi((i-1)r_{min})^2} - e^{-\lambda_{CH}\pi(ir_{min})^2}). \end{aligned} \quad (A.4)$$

The calculation of Eq. (A.4) can be represented with a simple integral operation, and then Eq. (5.2) is obtained as below.

$$\begin{aligned} E[N_{CM}^i] &= \lambda_{CM} 2\pi \left(\int_0^{ir_{min}} l e^{-\lambda_{CH}\pi l^2} dl - \right. \\ &\quad \left. \int_0^{(i-1)r_{min}} l e^{-\lambda_{CH}\pi l^2} dl \right), \\ &= \lambda_{CM} 2\pi \int_{(i-1)r_{min}}^{ir_{min}} l e^{-\lambda_{CH}\pi l^2} dl. \end{aligned} \quad (A.5)$$